Current Research (2023) Newfoundland and Labrador Department of Industry, Energy and Technology
Geological Survey, Report 23-1, pages 197-220

LITHOGEOCHEMICAL FEATURES OF CAMBRIAN BASALTS FROM WESTERN AVALON PENINSULA, AVALON TERRANE, NEWFOUNDLAND: ALKALINE MAGMATISM ALONG AN INHERITED FAULT ZONE

A. Mills and J.J. Álvaro[1]
Regional Geology Section
[1]Instituto de Geosciencias, Dr. Severo Ochoa 7, 28040 Madrid, Spain

ABSTRACT

New whole-rock lithogeochemical results for eleven Cambrian mafic rocks from western Avalon Peninsula (Newfoundland), including seven pillow basalt lavas, three mafic tuffs and one gabbro, are compared to available data on Cambrian mafic rocks from a previous study in the same area. The basalts are interbedded, and, locally, in apparent tectonic contact, with black shale and minor carbonate layers and lenses of the Manuels River Formation (Harcourt Group) at Chapel Arm, southern Trinity Bay. At Placentia Junction, 15 km to the south, mafic tuff is in fault contact with dark-grey to black shale probably belonging to the Miaolingian Chamberlain's Brook–Manuels River transition. Contact relationships of the gabbro have not been observed, but it either crosscuts, or is in fault contact with, red shales of the Terreneuvian to Cambrian Series 2, Adeyton Group. Previously documented fossil assemblages of the Manuels River Formation place the basalts in the biostratigraphic Paradoxides davidus *Zone of the Drumian Stage (absolute age of 504.5–500.5 Ma).*

All of these Cambrian mafic rocks have moderate Mg#'s, Zr/Ti ratios, and Ni and Cr concentrations indicating they are primitive magmas that experienced limited differentiation prior to emplacement. They are light rare-earth-element-enriched, alkaline, OIB-like basalts, having high Nb concentrations and high Nb/Yb and Ti/Y ratios. They likely formed as low-degree partial melts from a garnet lherzolite mantle source, as indicated by their high TiO_2/Yb, $(Sm/Yb)_{MN}$ and $(Tb/Yb)_{CN}$ ratios. The Cambrian basalts occur in a narrow north-trending linear (half-)graben, parallel to a north-trending, possibly Acadian thrust fault. The OIB-like chemical affinity of the magmas, the elongated orientation of the sedimentary basin in which they occur, and the presence of an adjacent (half-)graben-parallel fault are consistent with their eruption under extensional conditions, possibly along pre-existing, Neoproterozoic structures.

INTRODUCTION

The Avalon terrane in eastern Newfoundland is the largest exotic terrane in the Appalachian–Caledonian orogen (*e.g.*, Hibbard *et al.*, 2006; Pollock *et al.*, 2009) and comprises Neoproterozoic volcano-sedimentary sequences that are overlain by a lower Paleozoic, mixed (carbonate–siliciclastic) cover succession having a distinct Cambro-Ordovician faunal assemblage. Biogeographically, this assemblage has been termed the "Avalonian Faunal Province" (Landing, 1996), formerly referred to as the "Acado-Baltic" assemblage (*e.g.*, Murphy and Nance, 1989) or the "Atlantic faunal realm" (*e.g.*, Hutchinson, 1962; Wilson, 1966). Avalonia, which takes its name from the Avalon Peninsula in Newfoundland (Figure 1), is considered a composite terrane, comprising a collage of differing Neoproterozoic blocks that share a markedly similar Cambrian to Ordovician cover sequence (*e.g.*, Barr and White, 1996; Nance *et al.*, 2008). On the west side of the Atlantic Ocean, West Avalonia includes eastern Newfoundland and extends southwestward, outcropping in Nova Scotia and New Brunswick, to Cape Cod (Massachusetts) in the U.S.A. In Europe, East Avalonia includes southeastern Ireland, Wales, England, Belgium, the Netherlands, southern Denmark and part of northwestern Germany (Cocks and Fortey, 2009). Avalonia is commonly viewed as a microcontinent that separated from Gondwana with the opening of the Rheic Ocean beginning in the Furongian to Early Ordovician (*e.g.*, Murphy *et al.*, 2004, 2009; van Staal, 2007; Pollock *et al.*, 2009, 2012; van Staal *et al.*, 2020). Recent studies suggest that parts of Avalonia also experienced an earlier (Tonian) event, based on zircon age populations presumably derived from Baltica (*e.g.*, van Staal *et al.*, 2020; Thompson *et al.*, 2022; Kuiper *et al.*,

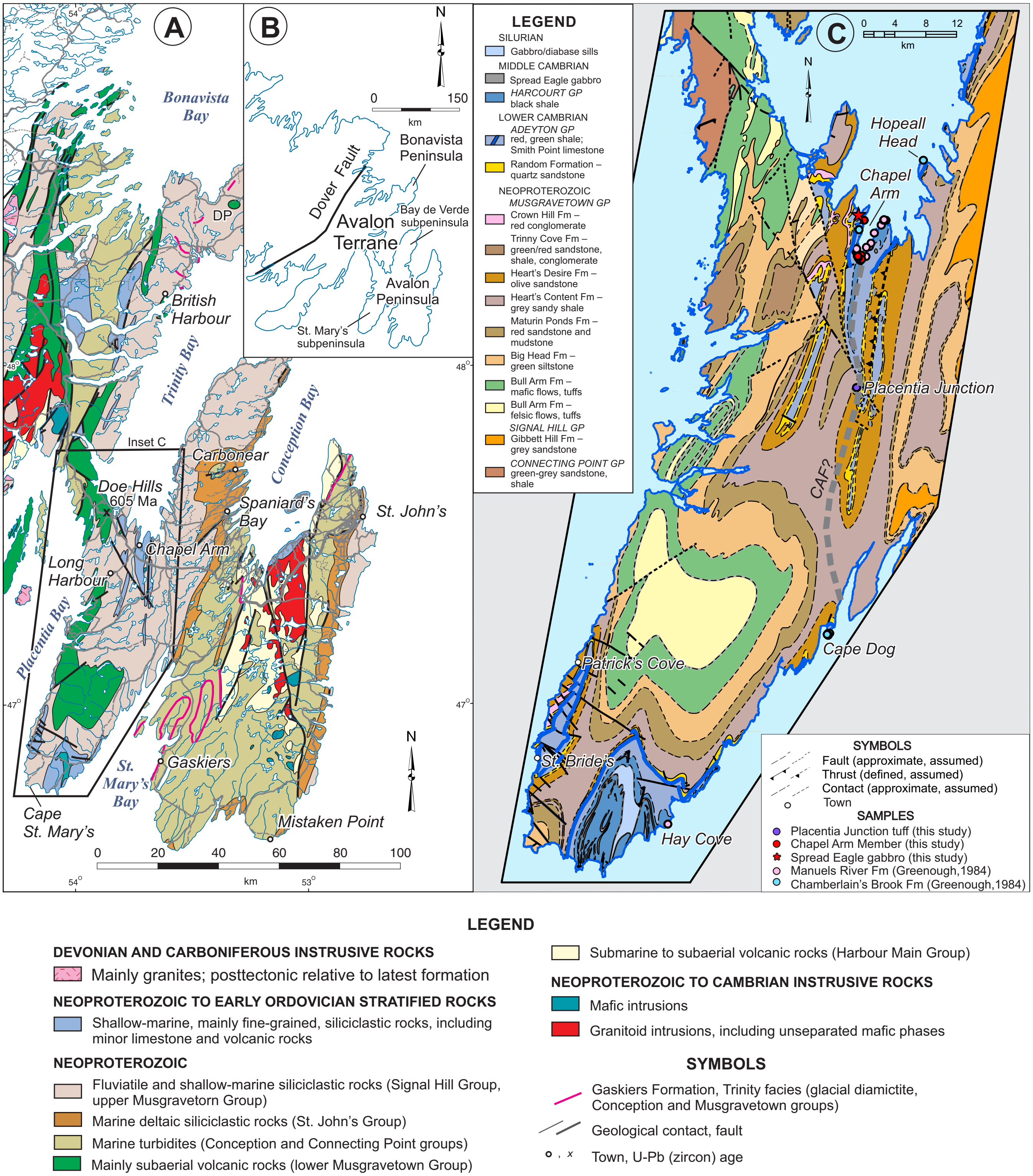

Figure 1. *A) Bedrock geology map for the eastern Avalon terrane in Newfoundland (modified from Colman-Sadd* et al.*, 1990); DP=Dam Pond; B) Insert map showing the extent of the Avalon terrane in Newfoundland and geographic areas referred to in the text; C) Bedrock geology map for the western Avalon Peninsula (after King, 1988); CAF?=proposed Chapel Arm Fault.*

2022), consistent with the proposed Baltic provenance for Avalonia based on isotopic evidence (*e.g.*, Thompson *et al.*, 2012; Henderson *et al.*, 2016). Intervening (Cryogenian) events remain cryptic.

The lower Paleozoic stratigraphy of the Avalon terrane in Newfoundland (herein referred to as Avalon) is underpinned by the work of Hutchinson (1962), built upon previous work by Howell (1925) and others, and based primarily on trilobite studies. Because the early subdivision of these units was based primarily on faunal content rather than lithology, Jenness (1963) proposed changes to make the stratigraphic framework more conducive to regional mapping. Broadly, these units include the lower Adeyton Group, comprising mainly green and red shale and slate with thin layers of limestone, and the upper Harcourt Group, comprising mainly dark-grey and black shale and slate. Jenness' (1963) stratigraphic framework has since been adopted for many regional mapping studies in Newfoundland's Avalonia (*e.g.*, King, 1988; O'Brien, 1994; Fletcher, 2006; Normore, 2010), and is adopted here to provide stratigraphic context for this study (Figure 2).

Whereas several geological investigations into Cambrian Avalon rocks have focused on fossils (Howell, 1925; Hutchinson, 1962; Poulsen and Anderson, 1975; Bergström and Levi-Setti, 1978; Martin and Dean, 1981, 1988), the mafic volcanic rocks that locally occur within the Cambrian sedimentary units have received little attention. Mafic volcanic rocks volumetrically comprise only a minor component of the Cambrian strata in Newfoundland, but their lithogeochemistry can provide insight into the tectonic setting for parts of the Cambrian rift sequence separating the Ediacaran Avalonian arc from the Early Ordovician drift of the terrane that led to the opening of the Rheic Ocean. To date, the only existing research into these rocks was conducted as part of a Ph.D. thesis (Greenough, 1984) that culminated in several publications on Cambrian mafic volcanism in Newfoundland, the Maritimes, and known global correlatives (Greenough and Papezik, 1985a, b, 1986). Relative to modern techniques, analytical methods at the time were somewhat limiting, in terms of detection limits, precision and accuracy, with some key elements not measured (*see* Methods section, below). As part of a reconnaissance-level Avalonian study, the authors visited outcrops of known Cambrian strata during the summer of 2022 with a two-fold sampling strategy: 1) to sample volcanic rocks to confirm previous interpretations of petrogenesis and geodynamic setting (*see* Greenough and Papezik, 1985a); and 2) to sample carbonate units within the strata for biostratigraphic and carbonate-productivity interpretations. Here we focus on the former, and present the first modern, whole-rock lithogeochemical data for Cambrian basalts from Avalonia in Newfoundland.

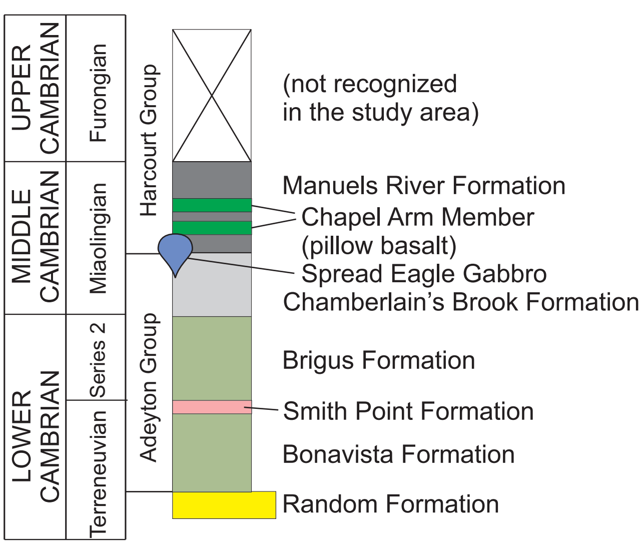

Figure 2. *Schematic stratigraphic section for Cambrian rocks of the Avalon Zone (modified after Landing, 2004).*

REGIONAL GEOLOGY

Neoproterozoic rocks west and east of the Chapel Arm area differ, both lithologically and stratigraphically. Rocks west of Chapel Arm have traditionally been assigned to the volcano-sedimentary Musgravetown Group (Hayes, 1948; Christie, 1950; McCartney, 1955, 1958, 1967), whereas rocks to the east were initially assigned to the sedimentary Hodgewater Group (Hutchinson, 1953; McCartney, 1967), but were re-assigned to the Musgravetown Group by King (1988), for his map compilation of the Avalon Peninsula of Newfoundland.

The oldest rocks in the area lie west of Chapel Arm and include Ediacaran bimodal volcanic rocks (Bull Arm Formation) and the overlying siliciclastic rocks of the Musgravetown Group (Hayes, 1948; Christie, 1950; Jenness, 1963; King, 1988; Figure 1C). Banded rhyolite at Doe Hills, west of Chapel Arm (Figure 1A), has been dated at 605 Ma (Mills *et al.*, 2021). At Long Harbour, mafic volcanic rocks included in the Bull Arm Formation are overlain by diamictite of the Big Head Formation (McCartney, 1967; Brückner, 1977) inferred to be correlative to the 580 Ma Trinity glaciogenic diamictite of the Musgravetown Group on the Bonavista Peninsula (Normore, 2011; Pu *et al.*, 2016; Mills and Sandeman, 2021b). No age constraints exist for rocks of the former Hodgewater Group, east of Chapel Arm (Bay de Verde subpeninsula of the Avalon Peninsula; Figure 1B). However, Ediacaran fossils at Spaniard's Bay (east side of Bay de Verde subpeninsula; Narbonne *et al.*, 2009; *see* Figure 1A) support the correlation of their shale beds with the Mistaken Point Formation, locally dated at 565 ± 3 Ma (Benus, 1988), 566.25 ± 0.35

Ma (Pu *et al.*, 2016) and 565.00 ± 0.16 Ma (Matthews *et al.*, 2020) near that type locality. The dark-grey shales of the former Carbonear Formation on the Bay de Verde subpeninsula (Hodgewater Group; Hutchinson, 1953; McCartney, 1967) were correlated based on lithology to those of the St. John's Group on Avalon Peninsula by King (1988), and the latter has been locally dated at 562.5 ± 1.1 Ma (Canfield *et al.*, 2020). Because the stratigraphy, overall, becomes younger from east to west across the Bay de Verde subpeninsula, concordantly and with no known structural imbrication (Hutchinson, 1953), King's (1988) Big Head Formation there (previously assigned to the Snows Pond Formation, Hodgewater Group, by Hutchinson (1953)) is likely younger than, and not correlative to, the Big Head Formation at its type locality near Long Harbour (Figure 1A). It is, therefore, plausible that a regionally significant fault, hitherto unrecognized, occurs in this western part of the Avalon Peninsula.

The oldest Cambrian unit on the Avalon Peninsula is the Terreneuvian ("lower Cambrian"; Figure 2) Random Formation (Hiscott, 1982; Landing, 2004). This unit varies up to 250 m in thickness and is characterized by thick-bedded quartz arenite and quartz conglomerate, commonly cross-stratified, and interpreted to reflect deposition on subtidal ridges or shoals (Hiscott, 1982). Typically, it is bounded by disconformities, except at Fortune Bay, where it conformably overlies the Chapel Island Formation, which spans the Ediacaran–Cambrian boundary (Landing, 1994).

The Random Formation is overlain by red, green and grey shale and slate, with lesser, commonly pink, limestone interbeds of the Adeyton Group (Jenness, 1963). In ascending order, the Adeyton Group includes the Bonavista, Smith Point, Brigus and Chamberlain's Brook formations. The first three of these are Terreneuvian to Cambrian Series 2 ("lower Cambrian" of Landing *et al.*, 2021; Figure 2) whereas the Chamberlain's Brook Formation is Miaolingian ("middle Cambrian") (Hutchinson, 1962; Jenness, 1963). The authors caution, as Jenness (1963) noted, that the thin limestone of the Smith Point Formation (~10 m average thickness; Jenness, 1963), should be treated as a member only, because the underlying and overlying shales, however faunally distinct (Hutchinson, 1962), are lithologically indistinguishable. Nevertheless, the distinctive lithology, colour and resistance to weathering (relative to the surrounding shales), make the Smith Point limestone a potential marker horizon within the several hundred metres of monotonous red, green and grey shale. The colour of the Bonavista/Brigus shale is also not consistent along strike, and so cannot be used to discern stratigraphic position (*see* also Mills, 2017). The issue with using the Smith Point limestone as a marker horizon is the assumption that limestones assigned to this unit formed broadly at the same time. Detailed paleontological work would need to be undertaken to test that disparate 'Smith Point-like' outcroppings constitute a single biozone. From a regional mapping perspective, this problem is further exacerbated by the presence of limestone layers in both the underlying Bonavista and overlying Brigus formations (McCartney, 1967) that could easily be taken for Smith Point limestone in the absence of fossil analysis.

The "lower Cambrian" Bonavista, Smith Point and Brigus formations are overlain by the Chamberlain's Brook Formation (Figure 2). The base of the Miaolingian Chamberlain's Brook Formation is marked by a basal manganiferous bed, ranging from 1 to 25 m thick, with MnO_2 and Fe_2O_3 cements encrusting shale to limestone strata (Hutchinson, 1962; Douglas, 1983). The manganiferous beds overlie a thin (2–3 cm) shale–pebble conglomerate, which, in conjunction with a recognized faunal break (Hutchinson, 1962), has been interpreted as an unconformity marking the Brigus/Chamberlain's Brook contact (Hutchinson, 1962; McCartney, 1967). The formation is thicker at western Trinity Bay, western St. Mary's Bay and eastern Placentia Bay, and thins both to the east and west (Hutchinson, 1962). Its lithology is mainly olive-grey to green shale (or slate), with nodules and thin beds of green, grey or pinkish limestone (Hutchinson, 1962). Hutchinson (1962) suggests that, where the basal manganiferous bed is missing, the contact with the underlying Brigus Formation can be drawn at the colour change from light-green and red shale to the darker olive-grey shale of the Chamberlain's Brook Formation. McCartney (1967) indicates that, in some areas, the upper one-third of the formation is dark-grey, difficult to distinguish lithologically from overlying black shale, and therefore combines the Chamberlain's Brook Formation with the Manuels River Formation to form a single "middle Cambrian" mappable unit (*e.g.*, McCartney, 1955, 1956, 1967).

The Manuels River Formation (Harcourt Group; Figure 2) conformably overlies the Chamberlain's Brook Formation. It comprises mainly black shale with thin beds and concretions of limestone, ranges between 20–30 m in thickness (Hutchinson, 1962), and is the youngest stratified unit in the study area. Pillow lava and breccia, referred to as the Chapel Arm Member (McCartney, 1967), occur intermittently within the Manuels River Formation (Figure 2) along a roughly north–south line between Hopeall Head to the north and Hay Cove to the south (*see* sample locations in Figure 1C). The Chapel Arm volcanic flows occur above the *Paradoxides bennetti* Zone, and within the *Paradoxides davidus* Zone (McCartney, 1967), corresponding to the Drumian Stage, with an absolute age between 504.5 and 500.5 Ma (Cohen *et al.*, 2022). Basalt flows also occur within the Chamberlain's Brook Formation (*e.g.*, at Cape Dog; *see* Figure 1C), although these are stratigraphically lower than the basalts of the Chapel Arm Member (Greenough and Papezik, 1985a, b).

A north–south trend is also defined by isolated outcrops of the Spread Eagle Gabbro (McCartney, 1967). Their spatial association with basalts of the Chapel Arm Member and local crosscutting relationships with "lower Cambrian" strata are consistent with the gabbros being feeders to the volcanic rocks of the Chapel Arm Member (McCartney, 1967; Greenough and Papezik, 1985a).

METHODS

Eleven rock samples were collected from Cambrian units from the western Avalon Peninsula (Figure 3). Two samples, one basalt and one gabbro, were collected from Norman's Cove, six basalt samples were collected from the south side of the community of Chapel Arm, and three mafic tuff samples were collected from near Placentia Junction, located ~15 km to the south (Figure 3). The basalts from Norman's Cove and Chapel Arm are all assigned to the Chapel Arm Member of the Manuels River Formation (McCartney, 1967). Each rock sampled was representative of the outcrop, free of veins and obvious alteration, and weathered surfaces were carefully removed. Thin section slabs and representative hand samples were collected and approximately 1 kg of clean, homogeneous rock fragments were then separated for whole-rock lithogeochemical analysis. Samples were processed and analyzed at the Geological Survey's geochemical laboratory. Sample preparation and analytical methods are outlined by Finch *et al.* (2018). The raw data were released to the public without interpretation (Mills, 2022). Sample locations are shown on Figure 3.

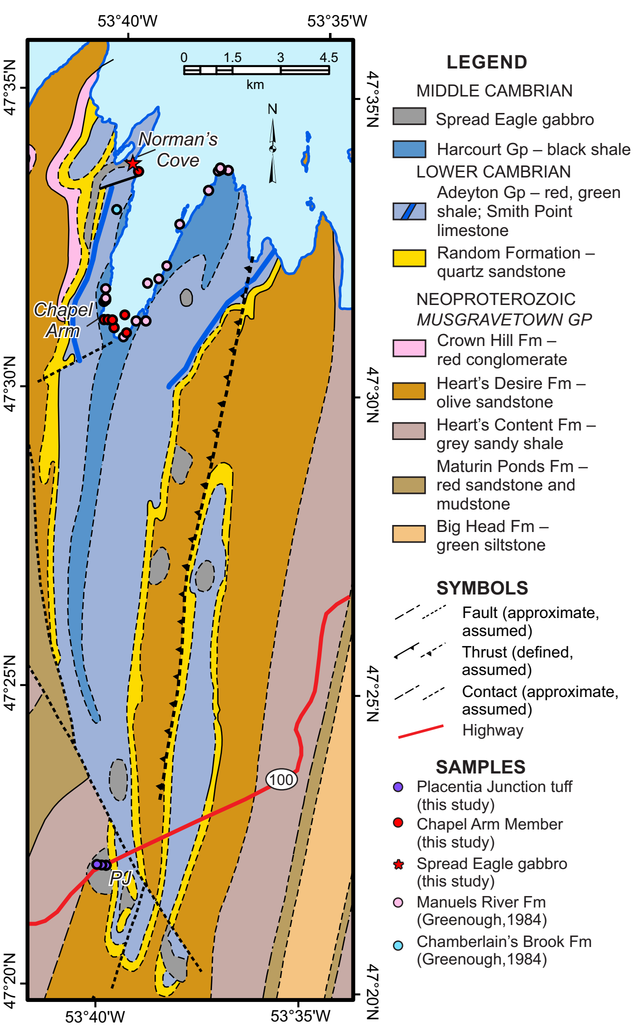

Figure 3. *Sample location map showing locations of rocks collected for this study as well as those of Greenough (1984). PJ=Placentia Junction.*

In addition, archival whole-rock lithogeochemical data for 29 mafic rock samples collected from Cambrian units in the western Avalon Peninsula area, or "St. Mary's Bay area" (Greenough, 1984), were compiled and plotted for comparison. These samples include lava, tuff and diabase from Cambrian units (Chamberlain's Brook and Manuels River formations) at Chapel Arm, Placentia Junction, St. Bride's, Patrick's Cove, Dog Cove and Hay Cove (Figure 1C; Greenough, 1984). Major-element content of these rocks was determined by atomic absorption spectrophotometry, and trace-element abundances were determined by X-ray fluorescence. An incomplete suite of rare-earth-element (REE) analysis was acquired for only six of the Greenough (1984) samples. Abundances of certain elements now routinely used in petrogenetic interpretation, including Hf, Ta, Tb, Ho and Lu, were not determined, likely owing to their low abundances with respect to detection limits of available analytical techniques. Nevertheless, the archival data of Greenough (1984) comprise a solid database with which the modern, but more limited dataset of the current study may be compared and are available on the Geological Survey of Newfoundland and Labrador's GeoAtlas (https://geoatlas.gov.nl.ca/).

FIELD DESCRIPTIONS

Cambrian mafic rocks were collected in three areas on the western Avalon Peninsula: Norman's Cove, Chapel Arm and Placentia Junction (Figure 1C). The first two of these are communities along the southern shore of Trinity Bay and the basalts at these locations are considered part of the Chapel Arm Member of the Manuels River Formation. The mafic tuff from Placentia Junction is treated separately based on its different lithology.

At Norman's Cove, gabbro outcrops on the north side of Norman's Cove River. Its contact relationships were not observed, and it either intrudes the red shales of the Adeyton

Group or effectively bounds the "lower Cambrian" strata due to its exploitation of a pre-existing fault (Plate 1A). The gabbro is medium grained and composed of pinkish tabular to equant feldspars that average 2 mm in length, with fine-grained dark material interstitial to the feldspars. South of the Norman's Cove River, two subvertical sections of pillowed basalts are intercalated with black shale and cm- to dm-scale dolostone interbeds of the Manuels River Formation. The first (northern and stratigraphically lowest) occurrence of basalt comprises large (1 x 3 m), slightly flattened pillows having large (>1 cm) carbonate amygdales (Plate 1B), whereas pillows of the second basalt (to the south and stratigraphically above) are more equant (1 x 1 m), have smaller amygdales (<1 cm), and appear less deformed. The latter flow was sampled for petrography and lithogeochemistry analyses.

At the southern end of Chapel Arm, 4.5 km south of Norman's Cove, basalt is interbedded with black shale, about 50 m above the concordant contact between steeply dipping dark-grey shales and black shales, likely the contact between Chamberlain's Brook and Manuels River formations, respectively. Near the contact between the black shale and basalt, beds steepen to subvertical, are highly cleaved and locally disrupted or brecciated. Limestone nodules are concentrated in some slumped and contorted beds (Plate 1C), indicating episodic syndepositional seismic disruptions. The intensity of deformation and role of tectonic imbrication are likely more important than previously recognized, as evidenced by cleavage-parallel tight to isoclinal folding (Plate 1D), and subtle fault planes separating similar shales having slightly different bedding orientations (Plate 1E). The contact between the black shale and basalt is sharp and appears faulted. Neither the magnitude nor sense of displacement was discerned. Farther east, along the shores of Chapel Arm, basalt outcrops are mainly pillowed (Plate 1F), and the black shale exhibits a variably developed, although commonly strong, cleavage. Down-dip slickenlines are locally visible on some bedding surfaces (Plate 1G). Lenses of carbonate occur locally (Plate 1H, I), as do framboidal pyrite aggregates of up to 2 cm diameter (Plate 1I).

Along Highway 100, south of the Trans-Canada Highway, a roadcut exposure was investigated near the turn-off to Placentia Junction (Figure 3). Dark-grey to black shale is exposed at the northeastern end of the roadcut. Based on colour features, the shale in this area should be part of the Chamberlain's Brook–Manuels River transition. A ~2-m-thick, brown-weathering, highly disrupted zone occurs near the contact with mafic tuff to the southwest (Plate 2A), obscuring the nature of the original contact. The true thickness of these highly disrupted rocks is likely much less than 2 m, as the main cleavage by which they are affected is oblique to the roadcut. The mafic tuff is typically structureless (massive), but a crude stratification occurs locally, particularly within the granule- to fine-grained, normal graded litharenites near the top of the bed sets (Plate 2B). Intervals containing cobble-sized medium-grey, mudstone clasts also occur locally (Plate 2C). The massive, tabular to lenticular beds are clast-supported, with subrounded to angular, mainly basaltic fragments, and carbonate occurs as an infill phase between the fragments. These pyroclastic or volcano-sedimentary strata typically have scoured bases and planar tops. Locally, the thick massive deposits are interbedded with thinning- and fining-upwards sets, up to 0.4 m thick, of clast-supported, granule- to fine-grained litharenites, with rounded to angular basalt-dominant grains set in a silty matrix. These stratified interbeds exhibit parallel to low-angle normal graded laminae and planar to wavy tops, small- to medium-scale low-angle crosslamination, and commonly have scoured basal contacts (Plate 2B).

PETROGRAPHIC DESCRIPTIONS

The gabbro from Norman's Cove contains ~65% feldspar, 25% amphibole, 8% opaque minerals and trace quartz, apatite and titanite. Feldspars are randomly oriented, euhedral to subhedral, appear turbid due to sausseritization, and average ~1–2 mm in length. Some feldspars contain inclusions (mainly amphibole), lending these crystals a poorly developed spongy texture. The amphibole occurs as felt-textured, angular polycrystalline aggregates interstitial to the feldspars (Plate 3A) and may be pseudomorphs of primary pyroxene. The opaque minerals are quadrate to rhombic in section and average ~200 μm. Rare quartz crystals are euhedral, exhibiting hexagonal sections and do not exceed 400 μm. (Their uniaxial positive interference figure confirms that these crystals are indeed quartz and not nepheline). Trace apatite crystals are euhedral and range up to 400 μm in length. Trace titanite crystals are equant, anhedral and <100 μm in size.

The basalt from Norman's Cove contains ~40% feldspar, 40% chlorite and 20% amygdales; the latter range up to 1 cm in diameter and are filled with prehnite and/or calcite (Plate 3B). Primary plagioclase, now albite, occurs mainly as randomly oriented laths ranging up to 300 μm. Most appear untwinned and skeletal crystals are locally preserved. Angular polycrystalline chlorite aggregates are common. Rare orthorhombic prisms up to 1 mm in length are preserved indicating that these are pseudomorphs after a primary mafic phase, probably pyroxene.

Basalts from the southern end of Chapel Arm are highly altered and primary minerals are not preserved. The groundmass ranges from dark and mottled (possibly originally glassy; Plate 3C) to plagioclase-rich with skeletal textures locally preserved (Plate 3D). Plagioclase laths are gen-

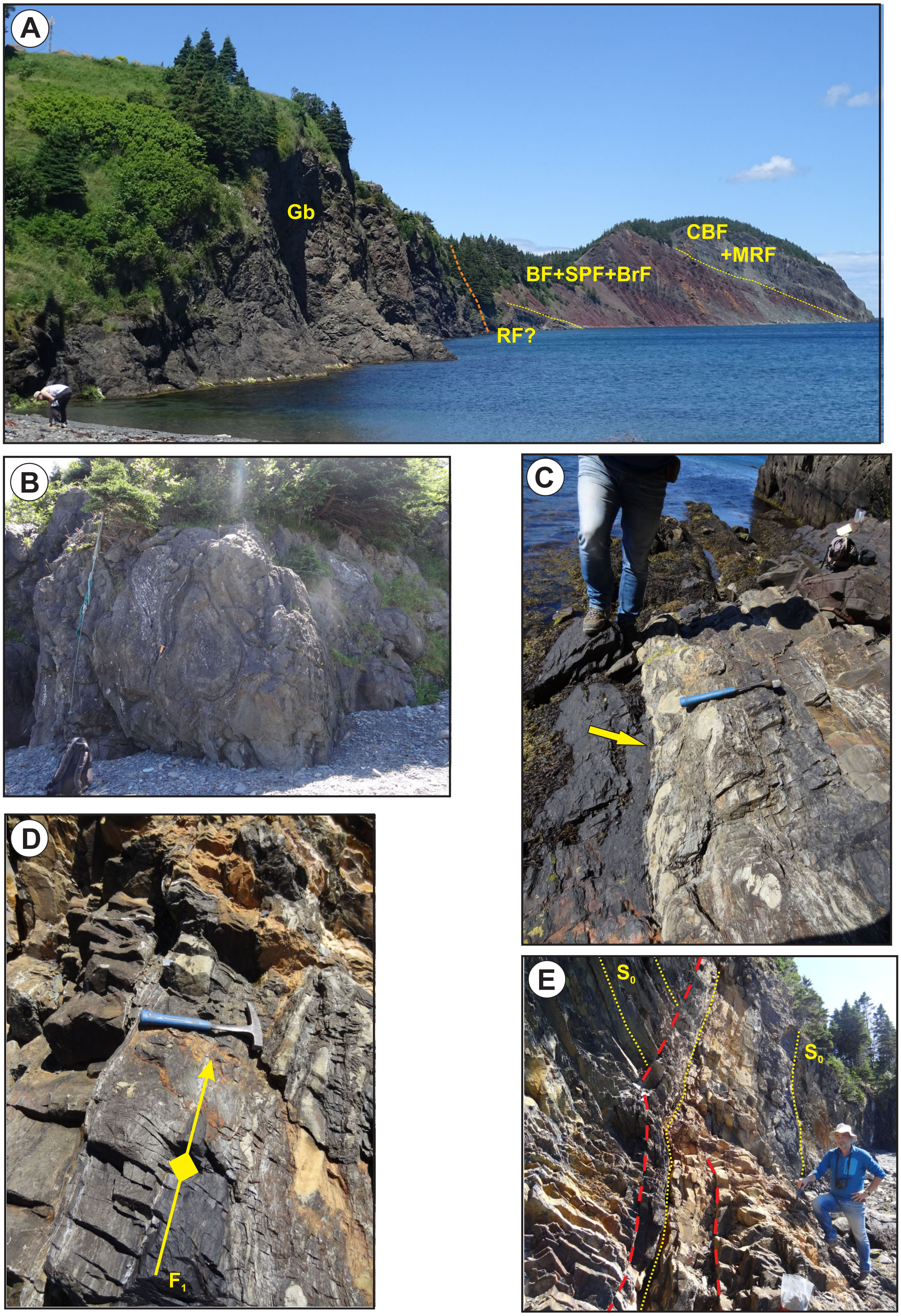

Plate 1. *Continued on next page.*

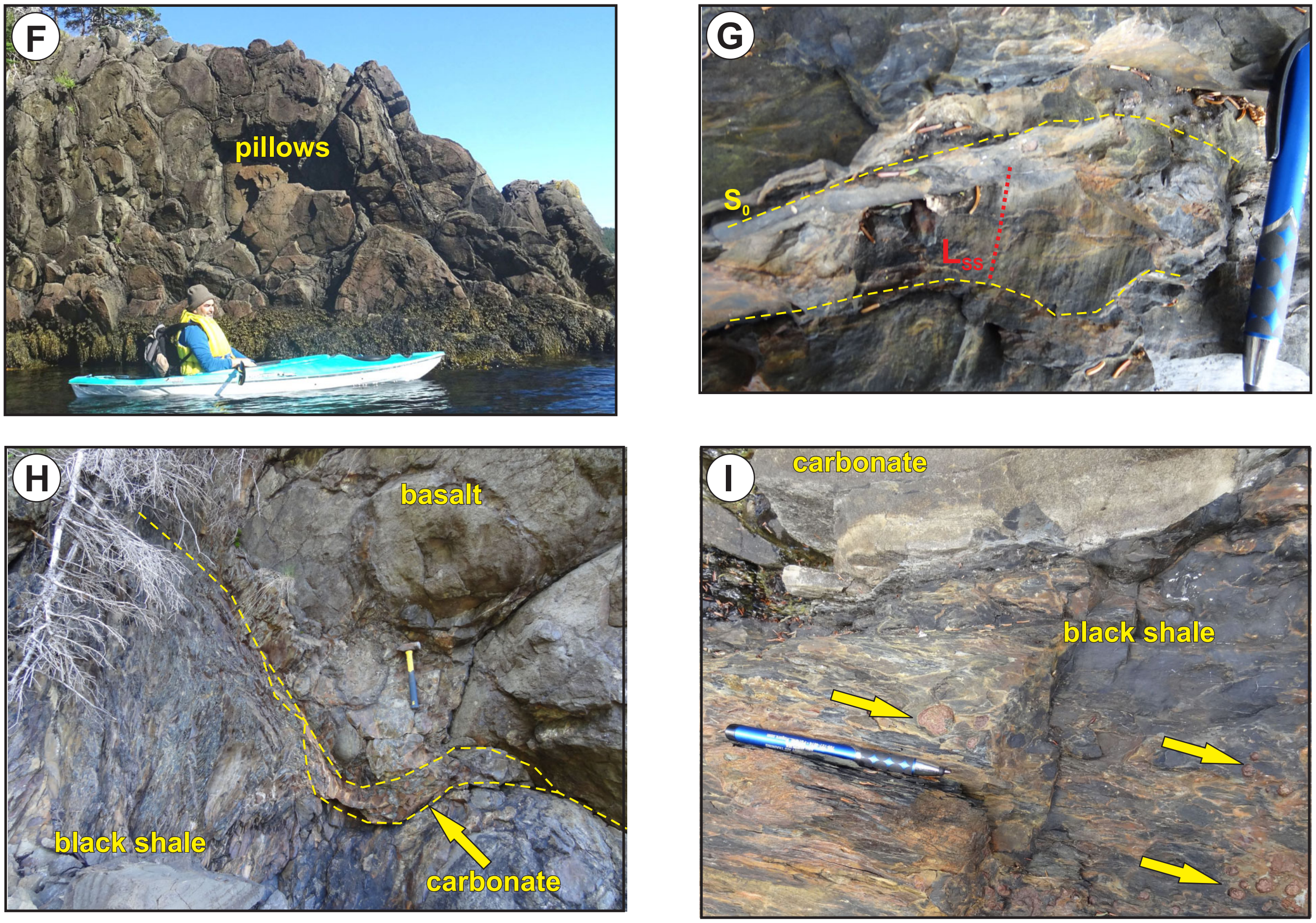

Plate 1. *Field photographs from Norman's Cove and Chapel Arm. A) Oblique view to the northwest from Norman's Cove River, showing gabbro intrusion (Gb), and Cambrian rocks exposed to the north (RF?=possible Random Formation; BF+SPF+BrF=Bonavista, Smith Point and Brigus formations, or some component(s) thereof; CBF+MRF=Chamberlains Brook and possibly Manuels River formations); B) Mega-pillows of coarsely amygdaloidal basalt, southeast of Norman's Cove River; C) Disrupted, slumped, carbonate-nodular bed (yellow arrow) intercalated with black shale of the Manuels River Formation at south end of Chapel Arm; D) Crest of apparently south-plunging anticline (yellow arrow) cored by Manuels River Formation black shale, with limbs of dark-grey shale, possibly of the underlying Chamberlains Brook Formation; E) View east of subvertical fault zone (red dashed lines) through intercalacted black shale and carbonate layers (tan coloured); note that bedding (yellow dashed lines; S_0) is parallel to the fault zone on the south (right-hand) side, but oblique to the fault on the north (left-hand) side of the fault; F) Pillowed basalt on west side of Chapel Arm; G) Steeply dipping slickenlines (LSS) on subvertical bedding surface along the west side of Chapel Arm; H) Deformed black shale and carbonate overlain by basalt; I) Competent carbonate lens (top) intercalated with well-cleaved black shale; note framboidal pyrite (yellow arrows) in the shale.*

erally fine grained (200–400 µm in length), randomly oriented, untwinned and slightly turbid. Skeletal laths occur locally. Chlorite occurs as irregularly shaped, fine-grained polycrystalline aggregates that range from <100 µm to >1 mm. Amygdales are generally carbonate-filled and range up to 1 cm in diameter (Plate 3D).

Mafic tuff from Placentia Junction comprises mainly angular basaltic fragments (Plate 3E, F) that range in size from <1 mm to >1 cm. Some fragments are dark and have a glassy appearance (Plate 3E), whereas others appear chlorite-rich and highly vesicular (Plate 3F). A network of dominantly calcite and quartz occurs between the fragments (Plate 3E). Of the three samples collected from Placentia Junction, one contains minor (~5%) siliciclastic fragments and these range from angular to rounded. Carbonate also occurs in veinlets cutting through both the fragments and quartz–carbonate infill. The matrix in the litharenite topping the bed sets comprises less than 10% by volume, and consists of silty–sandy rock fragments locally cemented by hematite.

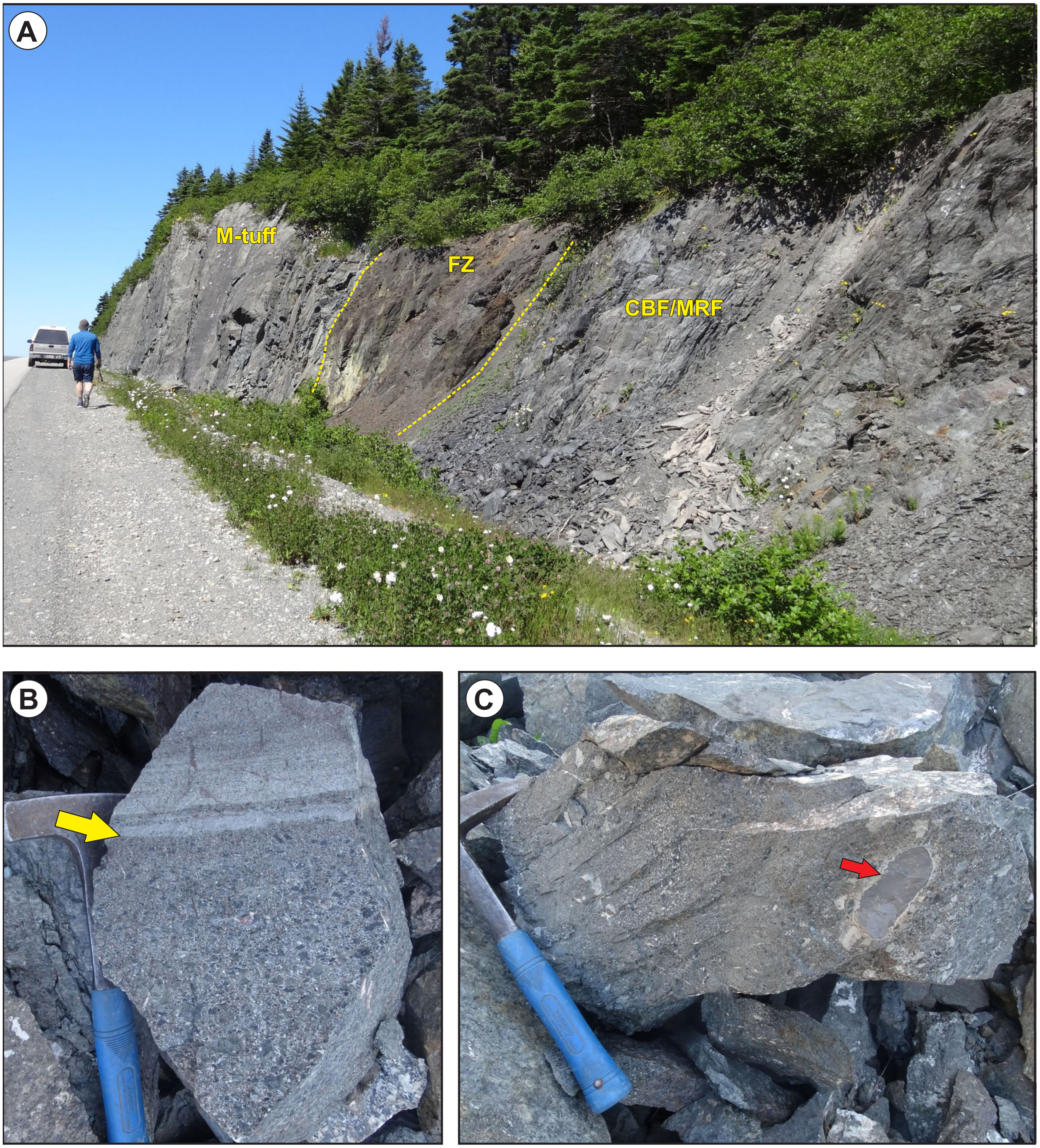

Plate 2. *Field photographs from Placentia Junction. A) View to the southwest near Placentia Junction showing brown-weathering fault zone (FZ) between highly cleaved dark-grey shale (Chamberlain's Brook Formation, CBF; and/or Manuels River Formation, MRF) and mafic tuff (M-tuff); B) Fining-upwards mafic tuff comprising subrounded to angular basaltic clasts, overlain by granule- to fine-grained litharenite (yellow arrow); C) Clast-supported mudstone clast in mafic tuff (red arrow).*

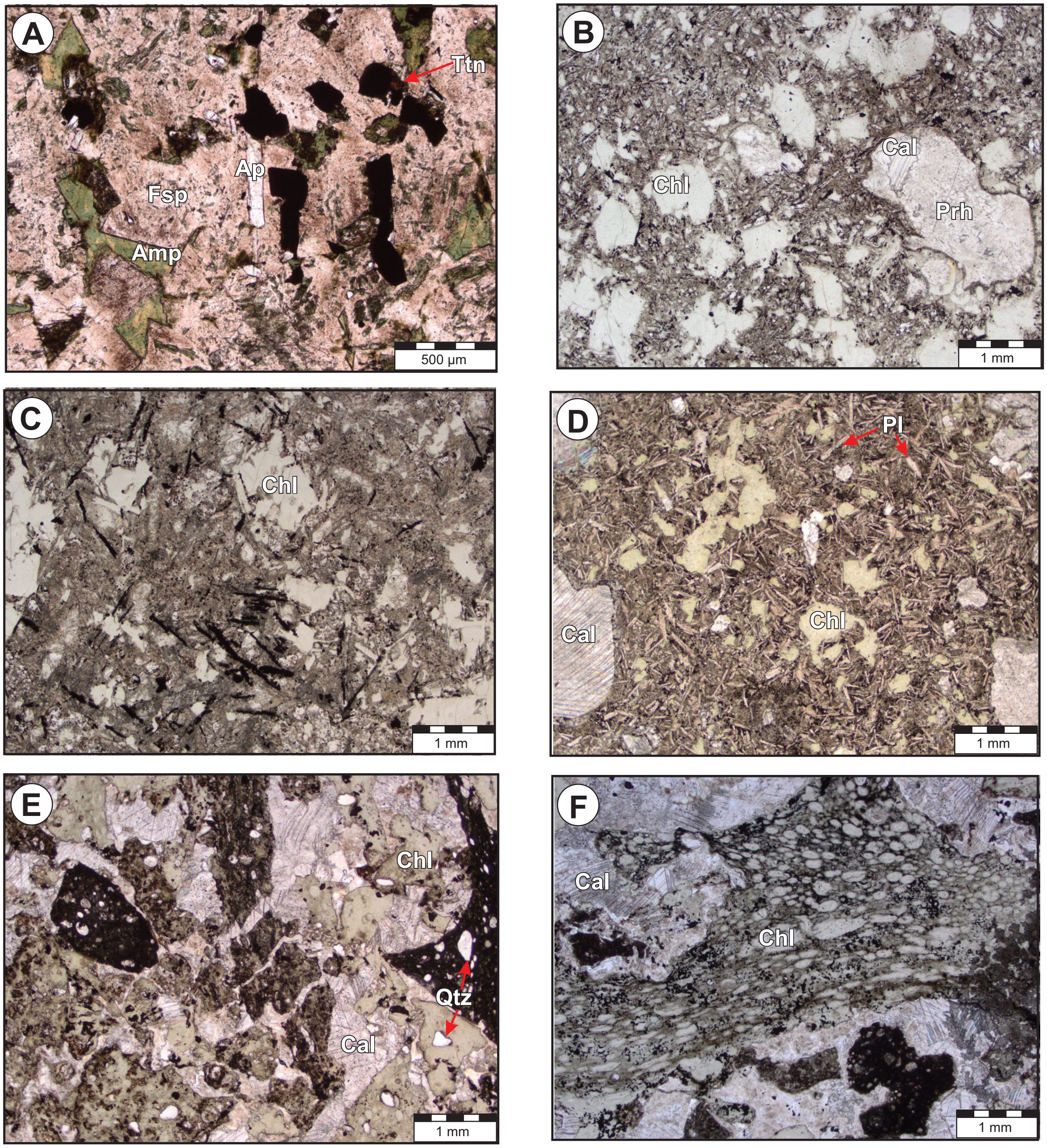

Plate 3. *Photomicrographs of Cambrian mafic rocks from Norman's Cove, Chapel Arm and Placentia Junction. A) Gabbro from Norman's Cove River showing turbid (altered) feldspar (Fsp), interstitial amphibole (Amp), opaque minerals, and accessory apatite (Ap) and titanite (Ttn); B) Pillow basalt from Norman's Cove, showing randomly oriented, altered feldspar laths in the groundmass, sub-equant pseudomorphs of chlorite (Chl), and amygdales filled with prehnite (Prh) and calcite (Cal); C) South Chapel Arm basalt, showing an altered groundmass (possibly originally glassy), with opaque minerals forming 1-m-long, fine linear aggregates, and chlorite (Chl) pseudomorphs; D) South Chapel Arm basalt showing randomly oriented feldspar (Pl) laths preserved in the groundmass, chlorite (Chl) likely pseudomorphing a mafic phase, and calcite (Cal) filling amygdales; E) Altered basaltic fragments are either glassy (vesicular fragments to the left and right of the center of field of view) or completely altered to chlorite (Chl), note the presence of quartz (Qtz) indicating the basalts are silica-saturated, coarse calcite (Cal) crystals form an infill network between basalt fragments; F) Highly vesicular basalt clast may originated as pumice. All photomicrographs are taken under plain-polarized light.*

LITHOGEOCHEMICAL RESULTS

ALTERATION AND ROCK CLASSIFICATION

In light of the alteration evident from both the petrographic observations and the alteration indices (Figure 4A), the Cambrian basalts are classified as alkali basalts, according to the Zr/Ti *vs.* Nb/Y discriminant (Pearce, 1996; Figure 4B), and further evaluation and interpretation of these rocks is based on select major elements (Al, Ti, Fe and P), high field strength elements (HFSE; Y, Th, Nb, Ta, Zr, Hf), the REE (except Ce and Eu) and transition metals (Cr, Ni, Co, Sc and V) as these elements are relatively immobile and typically remain unaffected during alteration and metamorphism.

The nature of the alteration affecting the Cambrian basalts is well illustrated by the alteration box plot of Large *et al.* (2001; Figure 4A). The CCPI (chlorite–carbonate–pyrite index), on the ordinate axis, measures the increase in MgO and FeO associated with chlorite development, which commonly replaces mafic minerals and feldspars in volcanic rocks (*e.g.*, Large *et al.*, 2001), resulting in a net loss of Na_2O and K_2O. None of our samples and only five of the 29 samples from Greenough (1984) fall within Large *et al.*'s (2001) least-altered-box (Figure 4A). These are the same ones that have 2–4% K_2O, with all other samples having <1% K_2O (Figure 5F). Those low-K_2O samples fall along the near-horizontal trend between epidote/calcite and chlorite/pyrite alteration on Large *et al.*'s (2001) box plot, indicating effects of both chlorite and carbonate alteration. This is consistent with abundant chlorite and calcite observed in these rocks in thin section.

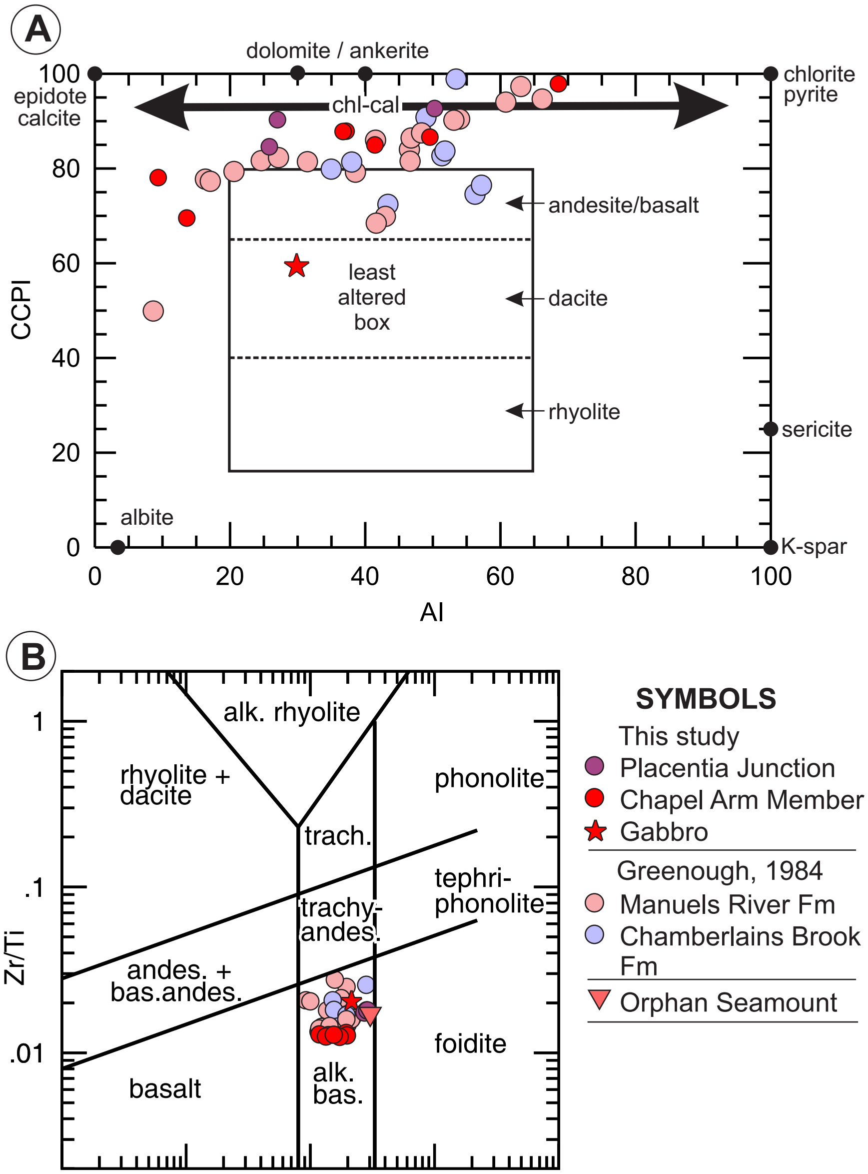

Figure 4. *Alteration and rock classification diagrams. A) Alteration box-plot (after Large* et al.*, 2001). CCPI=chlorite–carbonate–pyrite index; AI=Ishikawa alteration index; B) Rock classification diagram based on trace-element composition (Pearce, 1996).*

BINARY SYSTEMS/ FRACTIONATION TRENDS

On modified Harker diagrams, substituting Zr for SiO_2, the data generally appear to fall into three clusters or groupings. The Chapel Arm Member group (red circles) includes seven of the 11 samples collected for this study and 20 of the 29 Greenough (1984) samples (pink circles), the Chamberlain's Brook Formation group (light blue circles) includes nine of Greenough's (1984) samples, and the Placentia Junction group (purple circles) includes the three mafic tuff samples from Placentia Junction. A few samples are outliers, as they do not consistently fall within one of the three groups. Most of the major elements, such as Al_2O_3, Na_2O, FeO^T, and the minor elements P_2O_5 and TiO_2 increase (positive slope) with increasing Zr content (Figure 5), whereas CaO and MnO decrease (negative slope). No clear trend is evident with respect to

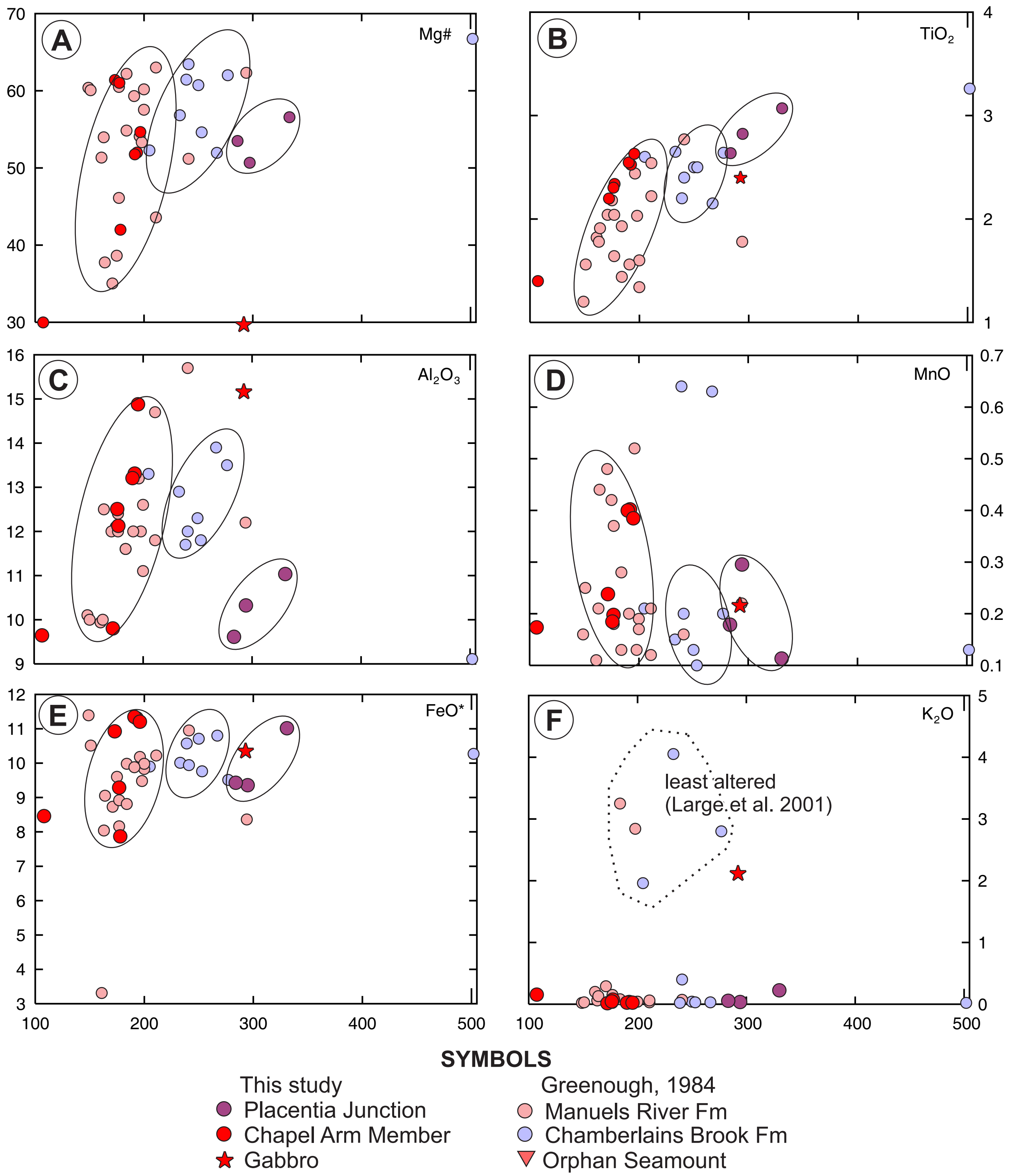

Figure 5. *Binary plots of samples collected for this study, and from Greenough's (1984) data. A) Mg# vs. Zr; B) TiO_2 vs. Zr; C) Al_2O_3 vs. Zr; D) MnO vs. Zr; E) FeO* vs. Zr (where total Fe is represented as ferrous iron); F) K_2O vs. Zr.*

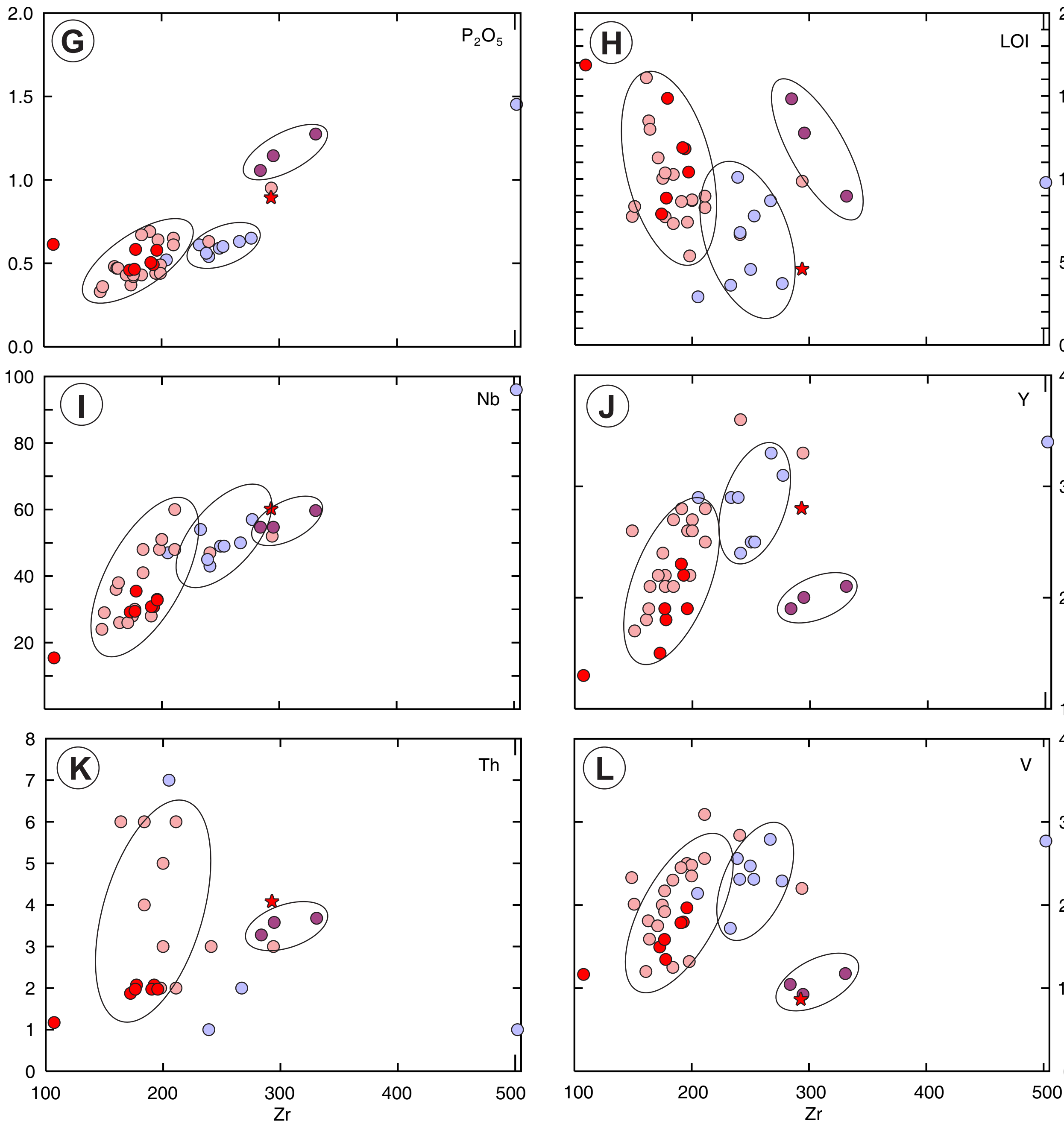

Figure 5 (continued). *Binary plots of samples collected for this study, and from Greenough's (1984) data. G) P_2O_5* vs. *Zr; H) LOI* vs. *Zr; I) Nb* vs. *Zr; J) Y* vs. *Zr; K) Th* vs. *Zr; L) V* vs. *Zr.*

$K_2$0, as most of the data fall very close to the abscissa, with only five of Greenough's (1984) samples and the gabbro collected for this study containing >1% K_2O. The loss on ignition (LOI) represents a measure of the volatile content and shows a negative trend for all groups. Most key trace elements, such as Nb, Y, Th, V and Cr, show positive fractionation trends, although the sparseness of data and steepness of some of the slopes of trends may affect these apparent trends.

Samples from all three of the groupings have moderate Mg#'s (30–66), as well as Cr (24–410) and Ni (49–261) concentrations (Figure 6; Table 1).

EXTENDED RARE-EARTH-ELEMENT PLOTS (XREEs)

The XREE patterns for all of the Cambrian basalts are steep, with significantly enriched light REEs (LREEs)

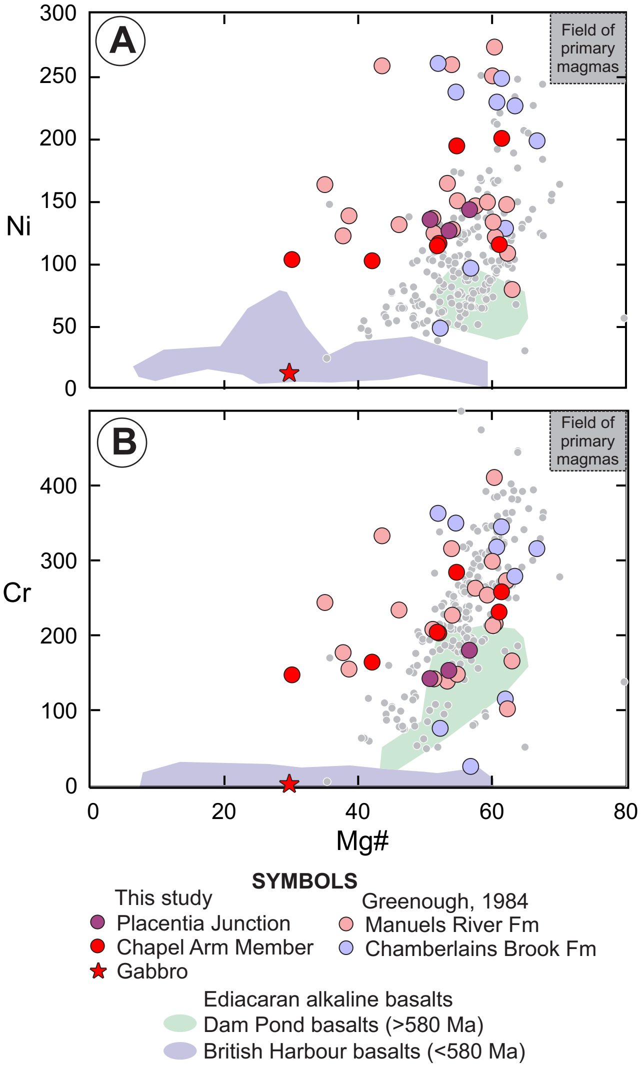

Figure 6. *Binary plots of samples collected for this study, and from Greenough's (1984) data, with approximate fields for primary mantle-derived melts (Roeder and Emslie, 1970; Ringwood, 1975), global, normal mid-ocean ridge basalts (grey dots; Lehnert* et al.*, 2000), and fields for Ediacaran alkali basalts (Mills and Sandeman, 2021a) shown for comparison. A) Ni* vs. *Mg#; B) Cr* vs. *Mg#.*

(Figure 7). The Greenough (1984) data are represented by a field, rather than individual analyses, because appropriate data are available for only six samples (two from the Manuels River Formation and four from the Chamberlain's Brook Formation) and Hf, Tb, Ho and Lu were not determined, resulting in gaps across which we have extrapolated the apparent XREE pattern. The new dataset is, overall, consistent with the historical data (Figure 7). Basalts from Placentia Junction are more LREE-enriched and have steeper XREE curves than those from the Manuels River Formation [average $(La/Yb)_{CN}$ for Placentia Junction = 39, whereas average $(La/Yb)_{CN}$ for Manuels River Formation = 12; CN denotes chondrite normalized, using normalizing values from Sun and McDonough, 1989; *see* Table 1]. The Placentia Junction samples also have La > Nb, whereas basalts of the Chapel Arm Member have La < Nb. All three Placentia Junction samples have negative Zr and Hf anomalies, whereas only one of the Chapel Arm samples has prominent negative Zr and Hf anomalies. The XREE pattern of the gabbro is similar to those for the Chapel Arm basalts in terms of its slope, shape, and its La/Nb ratio, and exhibits a very slight negative anomaly for Hf and Zr (Figure 7).

INTERPRETATION

The pillow basalts at Chapel Arm indicate a submarine volcanic setting. Slumped and contorted limestone beds interbedded with black shale indicate episodic syndepositional seismic disruptions. Cleavage-parallel, tight to isoclinal folding, and locally observed fault imbrication demonstrate that tectonic deformation is more important than previously recognized, both at Chapel Arm and Placentia Junction. At Placentia Junction, pyroclastic deposits display massive to bedded and lenticular geometries separated by dm-thick, normal graded litharenite interbeds having scoured basal contacts, normal graded laminae with parallel to low-angle crosslamination, and planar to wavy tops. Although primary dispersal of these thick, dominantly structureless deposits was probably related to sheet-wash or hyper-concentrated volcanogenic flows, the normal grading, parallel to low-angle crosslamination and planar to wavy tops of the interbedded litharenite indicate subsequent reworking. The aforementioned sedimentary structures, scarcity of matrix, geometry of bed sets, as well as grain size and shape, all suggest that these pyroclastic rocks were reworked, likely as marine channels and low-angle shoals, with dispersal induced by unidirectional bedload traction.

Chlorite and calcite are abundant secondary phases in the Chapel Arm basalts. Chlorite appears as possible pseudomorphs after primary pyroxene and in amygdales, whereas calcite appears both in amygdales and as an infill phase filling voids likely originally present in the pyroclastic rocks. Alteration of the Cambrian basalts is evident from both the alteration indices and the petrographic observations. Greenough and Papezik (1985b) investigated the alteration of Avalonian Cambrian basalts using mass-balanced calculations of least-altered *vs.* altered basalts, and concluded that two phases of alteration affected the rocks. The earliest phase resulted in chlorite formation, accompanied by the removal of K, Rb, Sr, Ba and Cu, and addition of Mn, Ga, V, Ni and Cr. Carbonate metasomatism followed, as shown by an increase in Ca, Sr and Na with increasing LOI, consistent with albitization of feldspar. Both chlorite and carbonate alteration may have occurred early following basalt eruption, as both phases are commonly associated

Table 1. Salient geochemical features of Cambrian basalts from the Avalon terrane (this study and Greenough, 1984) compared to Ediacaran alkali basalts (DP, BrHr) from the Bonavista Peninsula (Mills and Sandeman, 2021a)

	Cambrian Basalts				Ediacaran Basalts	
	This study		Greenough, 1984		Mills and Sandeman, 2021a	
Group/Series	PJ (n=3)	MRF (n=7)	MRF (n=20; n=2 for Y, REE)	CBF (n=9; n=4 for Y, REE)	DP (n=9)	BrHr (n=14)
Mg#	54	50	53	59	57	37
SiO_2	42	42	47	46	47.6	48.8
TiO_2	2.84	2.27	1.89	2.54	1.72	2.91
P_2O_5	1.16	0.5	0.52	0.68	0.58	1.09
Y	20	18	24	29	23	49
Ti	17026	13609	11331	15228	10298	17446
TiO_2/Y	851	756	472	525	448	356
Zr	303	174	190	274	184	381
Th	3.53	1.9	2.1	1.3	6.0	3.6
Nb	56	29	39	54	45	41
Cr	158	213	225	242	155	18
Ni	136	136	160	187	63	19
V	105	160	210	237	204	159
$(La/Yb)_{CN}$	39	12	10	22	13.77	6.61
$(La/Sm)_{CN}$	2.7	2	1.3	1.4	4.05	2.15
$(Gd/Yb)_{CN}$	8.1	3.8	5.8	8.3	2.12	2.18
$(Th/La)_{CN}$	0.51	0.75	0.43	0.89	1.12	0.70
$(La/Nb)_{CN}$	1.03	0.76	0.42	0.4	1.01	1.12
$(Th/Nb)_{CN}$	0.53	0.56	0.19	0.33	1.12	0.76
$(Sm/Yb)_{CN}$	14.44	5.78	8.26	7.41	3.40	3.09
$(Tb/Yb)_{CN}$	5.02	2.64	N/A	N/A	1.67	1.78
$(Sm/Yb)_{CN}$	9.52	8.1	8.25	7.4	3.40	3.09
sumREE	288	124	78	140	210	276

Note: PJ=Placentia Junction; MRF=Manuels River Formation; CBF=Chamberlain's Brook Formation; DP=Dam Pond basalts; BrHr=British Harbour basalts; CN=chondrite-normallized (normalization factors as per Sun and McDonough, 1989)

with low-temperature hydrothermal alteration fluids mixed with seawater (*e.g.*, Menzies and Seyfried, 1979; Andjić *et al.*, 2022).

The moderate Mg#'s, Zr/Ti ratios, and Ni and Cr concentrations (Table 1 and Figure 6) indicate that, although these Cambrian basalts do not represent primary mantle melts, they have apparently undergone very modest differentiation prior to eruption at surface, and are quite primitive (*e.g.*, Roeder and Emslie, 1970). In general, the basalts from the Chamberlain's Brook Formation have slightly higher Mg#, and Cr, Ni and V contents, and are therefore more primitive than those of the Manuels River Formation (Table 1). The Cambrian basalts are also more primitive than most of the alkali Ediacaran basalts from the Bonavista Peninsula (Figure 6; *see* Mills and Sandeman, 2021a).

High Nb contents, as well as Nb/Yb and Ti/Y ratios, indicate the Cambrian basalts are alkali, OIB-like, or 'within-plate' basalts (Figure 8A–F; Table 1; *e.g.*, Pearce, 1996). They are strongly LREE-enriched and the shapes and slopes of their multi-element patterns are similar to those of OIB, the Orphan Seamount and alkaline lamprophyres (Figure 7: Sun and McDonough, 1989; Pe-Piper *et al.*, 2013; Delor and Rock, 1991). Their TiO_2/Yb and Zr/Nb ratios are consistent with an OIB-like source, deeper than both normal and enriched mid-ocean ridge basalt sources (NMORB and EMORB, respectively; Figure 8C, F). Their high $(Sm/Yb)_{MN}$ and $(Tb/Yb)_{CN}$ ratios (MN = mantle-normalized; CN = chondrite-normalized; Table 1) also indicate a deep source, within the garnet stability field (Niu *et al.*, 2011; Rooney, 2010; Figure 8E). The source for such basalts must reside in the asthenosphere, below the lithospheric mantle (Niu *et al.*, 2011). Their Th contents and Th/Nb ratios are consistent with very little crustal or lithospheric contamination (Figure 8D; Pearce, 2008). The deep source, negligible contamination and modest fractionation indicate that the Cambrian basalts did not reside long in a lithospheric magma chamber

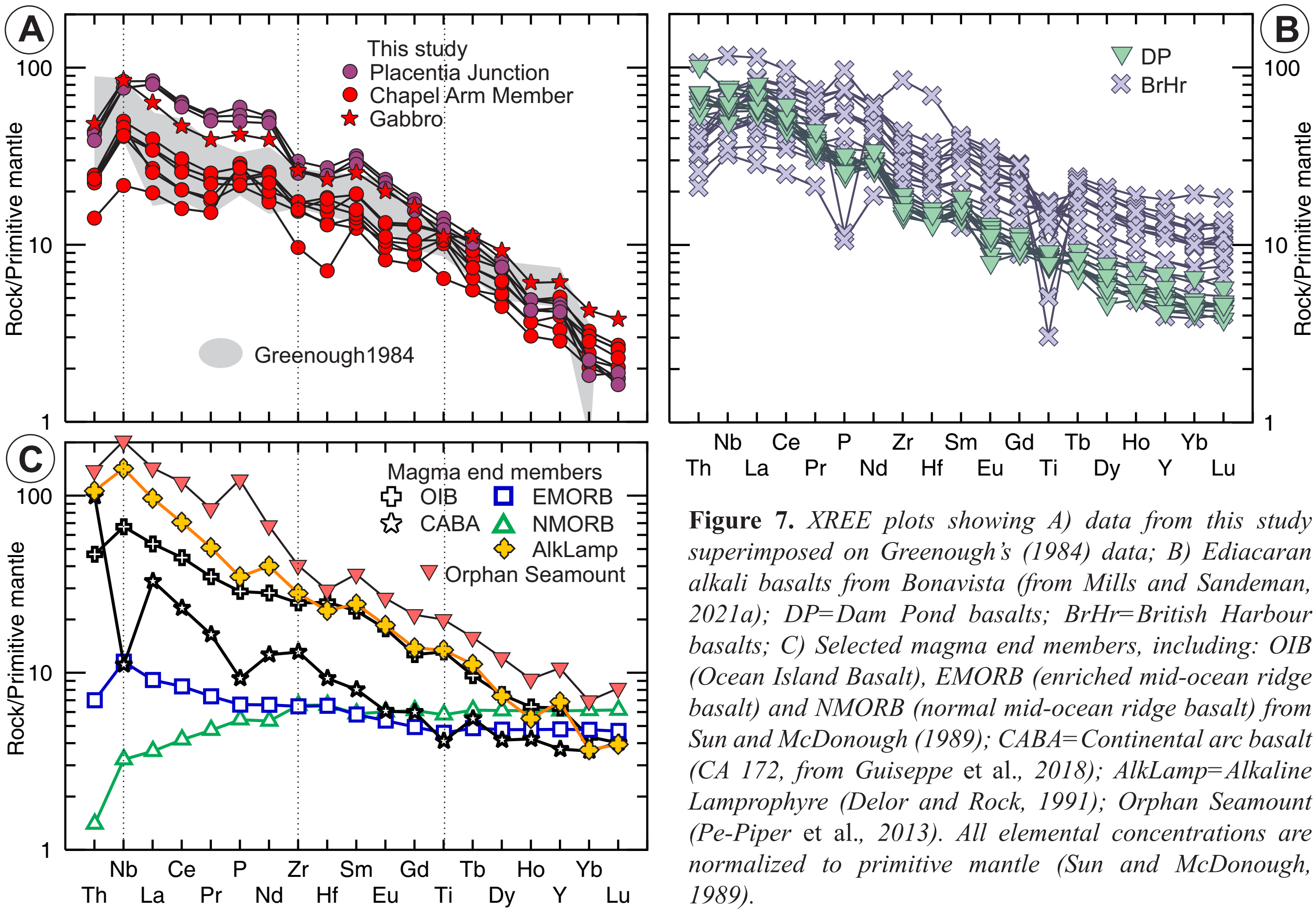

Figure 7. *XREE plots showing A) data from this study superimposed on Greenough's (1984) data; B) Ediacaran alkali basalts from Bonavista (from Mills and Sandeman, 2021a); DP=Dam Pond basalts; BrHr=British Harbour basalts; C) Selected magma end members, including: OIB (Ocean Island Basalt), EMORB (enriched mid-ocean ridge basalt) and NMORB (normal mid-ocean ridge basalt) from Sun and McDonough (1989); CABA=Continental arc basalt (CA 172, from Guiseppe* et al.*, 2018); AlkLamp=Alkaline Lamprophyre (Delor and Rock, 1991); Orphan Seamount (Pe-Piper* et al.*, 2013). All elemental concentrations are normalized to primitive mantle (Sun and McDonough, 1989).*

prior to eruption, and likely had a relatively direct route to the surface; a pre-existing structure may have provided such a conduit. Tb/Yb ratios of the Chapel Arm Member basalts indicate that they are the product of low-degree partial melting (possibly ~4%; Figure 9A) of a peridotite from the garnet–spinel transition zone (Figure 9B; MacDonald *et al.*, 2001). The mafic tuff from Placentia Junction shows a similar, OIB-like chemical affinity to that of the Chapel Arm basalts, but the former have steeper XREE patterns, higher La/Yb, Gd/Yb, Ce/Y, Tb/Yb ratios and ΣREE. They likely originated from low-degree melts of an enriched, more garnetiferous, and possibly more deeply rooted source relative to the Chapel Arm basalts (Table 1; Figures 8 and 9).

PLUME *VS.* EXTENSIONAL ENVIRONMENT

Alkali, or 'within-plate', magmatism has been linked to such settings as extensional zones, regions of lithospheric weakness (*e.g.*, suture zones), and mantle plumes (*e.g.*, Matton and Jébrak, 2009). Mantle plumes and extensional settings have been invoked as mechanisms for lithospheric rifting and/or continental breakup (*e.g.*, Bédard, 1985; Matton and Jébrak, 2009; Miranda *et al.*, 2009; Pe-Piper *et al.*, 2013; Álvaro *et al.*, 2022). A deep mantle plume, however, would be accompanied by distinct surface expressions such as early domal uplift and radial dyke swarms or rift structures associated with alkaline magmatism, and the volume of magma would be large (*e.g.*, Hawaiian Islands). In contrast, extensional processes cause lithospheric necking (*e.g.*, Mohn *et al.*, 2012), which would facilitate the passive rise of asthenosphere, resulting in adiabatic decompression melting (Bédard, 1985; Matton and Jébrak, 2009). An extensional model therefore predicts subsidence, rather than doming, and low-volume magmatism, particularly focused along pre-existing structures (Bédard, 1985; Matton and Jébrak, 2009).

The Cambrian basalts investigated here are interpreted in the context of crustal or lithospheric extension. The changing depositional setting of stratigraphic succession from the offshore-dominant Chamberlain's Brook green shales to the kerogenous offshore to basinal Manuels River black shales reflects a significant marine transgression (*e.g.*, Landing *et al.*, 2022), which is more consistent with subsidence than doming. Whereas no regional normal (extensional) faults, synsedimentary or tectonic, are present on extant maps of

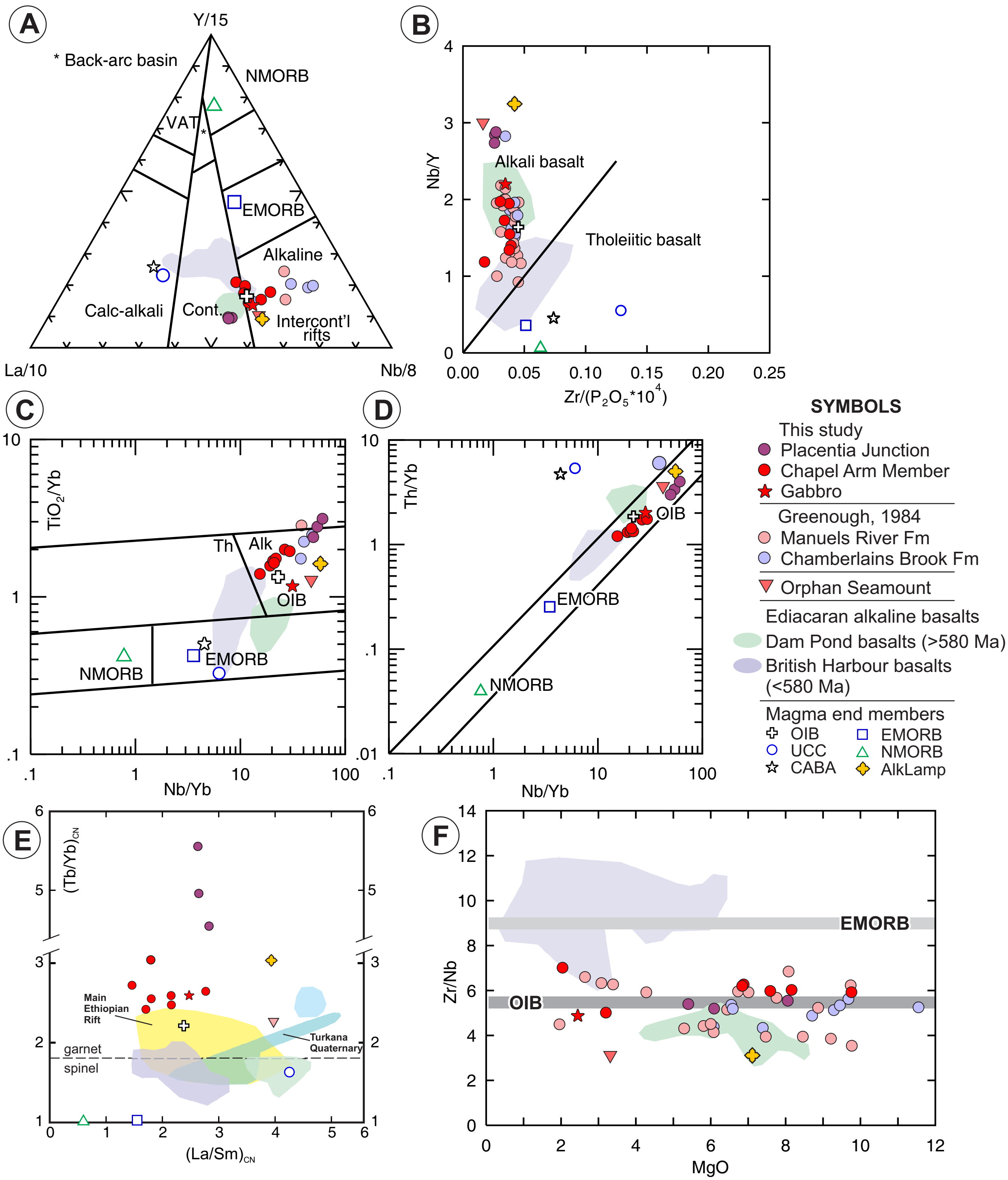

Figure 8. *Discrimination diagrams based on trace elements and trace-element ratios. A) Ternary plot of La–Nb–Y (after Cabanis and Lécolle, 1989); B) Nb/Y* vs. *Zr/P_2O_5 (after Floyd and Winchester, 1975); C) TiO_2/Yb* vs. *Nb/Yb (after Pearce, 2008); D) Th/Yb* vs. *Nb/Yb (after Pearce, 2008); E) $(Tb/Yb)_{CN}$ vs. $(La/Sm)_{CN}$ with fields for Main Ethopian Rift and Turkana Quaternary volcanic rocks and line for garnet- vs. spinel-dominated melting (from Rooney, 2010 and references therein); F) Zr/Nb* vs. *MgO with average OIB and EMORB (from Sun and McDonough, 1989) shown as lines. CN denotes chondrite-normalized. (values from Sun and McDonough, 1989).*

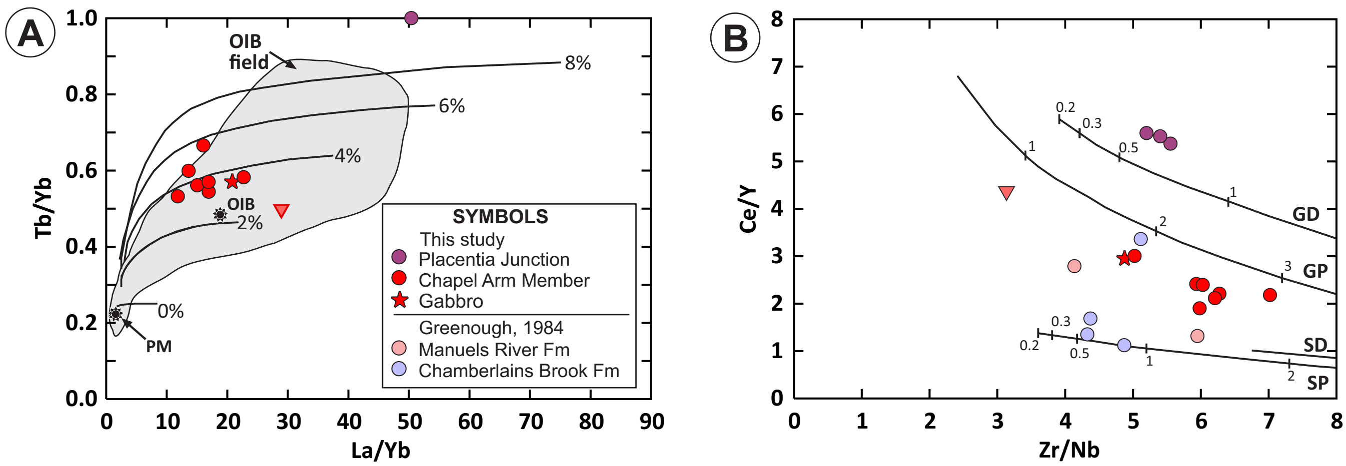

Figure 9. *A) Tb/Yb vs. La/Yb plot of Cambrian basaltic rocks from this study, with field of ocean-island basalts (OIB) for comparison. Lines represent melting of fertile lherzolite mantle, with amount of modal garnet indicated (after MacDonald* et al.*, 2001). Average OIB, PM (primitive mantle) are from Sun and McDonough (1989); B) Ce/Y* vs. *Zr/Nb plot of Cambrian basaltic rocks. The lines represent non-modal fractional melting curves for four mantle compositions: GD=depleted garnet lherzolite; GP=primitive garnet lherzolite; SD=depleted spinel lherzolite; SP=primitive spinel lherzolite. Numbers on lines refer to percentages of melt (after MacDonald* et al.*, 2001 and references therein).*

Avalon, regional-scale faults of unknown type and sense are abundant both onshore (King, 1988) and offshore (Miller and Singh, 1995), and include four main trends: northwest-, north-, northeast- and east–west trending.

The Cambrian basalts of the Avalon occur in a narrow, north-trending linear (half-)graben, paralleled by the trend defined by disparate occurrences of the Spread Eagle gabbro and a north-trending linear reverse fault zone (Figure 1). The age and nature of these faults are not clear, however, the offshore magnetic and gravity data were previously interpreted to reflect the oldest, or Precambrian, fabric of the area (Miller and Singh, 1995). The confluence of the elongate north-trending orientation of the (half-)graben, the parallel lineament defined by the distribution of Spread Eagle gabbro occrences, and the presence of a nearby north-trending thrust fault are consistent with the presence of a significant, (crustal-scale?) pre-existing fault structure.

The current map compilation (King, 1988) correlates the Big Head Formation (lower Musgravetown Group) with siliciclastic units above proposed correlatives of the St. John's and Signal Hill groups on the Bay de Verde subpeninsula (Figure 1B, C). However, the Big Head Formation at its type locality southwest of the current study area contains glacial diamictite (Mills and Sandeman, 2021b) that is inferred to correlate with the 580-Ma Trinity facies on Bonavista Peninsula to the north (Normore, 2011; Pu *et al.*, 2016). If this correlation is correct, then this *ca.* 580 Ma unit cannot sit stratigraphically above a correlative of the *ca.* 562 Ma St. John's Group (Canfield *et al.*, 2020) on the east side of this fault (*see* also discussion in Regional Geology). There is no evidence for thrust faults on extant maps of Avalon that can account for the older Big Head Formation sitting structurally above rocks correlative to the younger St. John's and Signal Hill groups. The simplest explanation for this apparent stratigraphic discrepancy is that the lithological correlation of the Big Head Formation on southwestern Avalon with Hutchinson's (1953) Whiteway Formation (former Hodgewater Group) is incorrect. Lithological correlation between distinctive glacial deposits on Avalon has been corroborated locally by U–Pb (zircon) geochronology (Gaskiers Formation, Conception Group on Avalon Peninsula and Trinity facies of Musgravetown Group on Bonavista Peninsula; Pu *et al.*, 2016). The lithologically distinct diamictite is a more robust candidate for lithological correlation than the unremarkable green-grey siltstones of McCartney's (1967) Big Head Formation and Hutchinson's (1953) Whiteway Formation. We propose that the units on the southwest side of a Precambrian 'Chapel Arm Fault' (Isthmus and St. Mary's subpeninsula) are older than lithologically similar units on the northeast side (Bay de Verde subpeninsula; *see* Figure 1B, C), and the cryptic north-trending fault zone separating the two areas is of greater regional importance than previously recognized.

CONCLUSIONS

Cambrian basalts of the Chapel Arm Member are interbedded with black shales of the Manuels River Formation (Harcourt Group), deposited within the biostratigraphic *Paradoxides davidus* Zone (Hutchinson, 1962; McCartney, 1967) of the Drumian Stage, with an approximate absolute age of between 504.5 to 500.5 Ma (Cohen *et* *al.*, 2022). Slumped and contorted limestone beds, interbedded with the black shale, reflect episodic syndepositional seismic disruptions. Cleavage-parallel, tight to isoclinal folding, and local fault imbrication indicate that tectonic deformation is more important than previously recognized. Pyroclastic dispersal at Placentia Junction was probably due to sheet-wash or hyper-concentrated volcanogenic flows, with subsequent reworking by marine benthic currents, marine channels and low-angle shoals as indicated by local scours, normal grading, scarcity of matrix material and inclusion of mudstone clasts.

The similarity in shape and slope of the XREE pattern for the gabbro at Norman's Cove and the Chapel Arm basalts is consistent with the former being a feeder pipe to the latter.

Geochemical results suggest that all of the Cambrian mafic rocks are relatively primitive, as indicated by their moderate Mg#'s, Zr/Ti ratios, and Ni and Cr concentrations. These rocks are LREE-enriched and have multi-element patterns similar to those of OIB, the Orphan Seamount and alkaline lamprophyres. They originated as low-degree partial melts from a garnet lherzolite, OIB-like source. Their deep source, negligible contamination and modest fractionation indicate that the Cambrian basalts ascended quickly with limited lithospheric involvement. These rocks are interpreted to have formed in a magma-poor, rift-related extensional setting, likely along an, as yet, unidentified pre-existing north-trending Neoproterozoic fault zone. This cryptic fault zone may separate previously (and erroneously) correlated, lithologically similar units which are, in fact, spatiotemporally and stratigraphically distinct.

ACKNOWLEDGMENTS

Chris Finch and staff at the Geological Survey's geochemical laboratory provided timely delivery of quality lithogeochemistry data. Map figures were constructed by Charmaine Hamlyn. Dr. Alana Hinchey and Dr. Hamish Sandeman critically reviewed the manuscript and provided suggestions for improvement. Layout and typesetting were completed by Joanne Rooney.

REFERENCES

Álvaro, J.J., Pour, M.G., Sánchez-García, T., Zadeh, M.-R., K.-e., Hairapetian, V. and Popov, L.E.
2022: Stratigraphic and volcanic signatures of Miaolingian-Late Ordovician rift pulses in the Alborz Mountains, northern Iran. Journal of Asian Earth Sciences, Volume 233. https://doi.org/10.1016/j.jseaes.2022.105240

Andjić, G., Zhou, R., Buchs, D.M., Aitchison, J.C. and Zhao, J.
2022: Paleozoic ocean plate stratigraphy unraveled by calcite U-Pb dating of basalt and biostratigraphy. Communications Earth and Environment 3, Article 113. https://doi.org/10.1038/s43247-022-00446-1

Barr, S.M. and White, C.E.
1996: Contrasts in late Precambrian-early Paleozoic tectonothermal history between Avalon composite terrane sensu stricto and other possible peri-Gondwanan terranes in southern New Brunswick and Cape Breton Island, Canada. *In* Avalonian and Related Peri-Gondwanan Terranes of the Circum-North Atlantic. *Edited by* R.D. Nance and M.D. Thompson. Geological Society of America, Special Paper 304, pages 95-108.

Bédard, J.H.
1985: The opening of the Atlantic, the Mesozoic New England Igneous Province, and mechanisms of continental breakup. Tectonophysics, Volume 113, pages 209-232.

Benus, A.P.
1988: Sedimentological context of a deep-water Ediacaran fauna (Mistaken Point, Avalon Zone, eastern Newfoundland). *In* Trace Fossils, Small Shelly Fossils and the Precambrian–Cambrian boundary. *Edited by* E. Landing, G.M. Narbonne and P. Myrow. The University of the State of New York, Bulletin 463, pages 8-9.

Bergström, J. and Levi-Setti, R.
1978: Phenotypic variations in the Middle Cambrian trilobite *Paradoxides davidis* Salter at Manuels, SE Newfoundland. Geologica et Palaeontologica, Volume 12, pages 1-40.

Brückner, D.
1977: Significance of new tillite finds for east-west correlation of Proterozoic Avalon-zone formations in southeastern Newfoundland (Canada). Estudios Geológicos, Volume 33, pages 95-102.

Cabanis, B. and Lécolle, M.
1989: Le diagramme La/10-Y/15-Nb/8: un outil pour la discrimination des series volcaniques et la mise en evidence des processus de mélange et/ou de contamination crustale. Comptes Rendus de l'Académie des Sciences (Séries II), Volume 309, pages 2023-2029.

Canfield, D.E., Knoll, A.H., Poulton, S.W., Narbonne, G.M. and Dunning, G.R.
2020: Carbon isotopes in clastic rocks and the Neoproterozoic carbon cycle. American Journal of Science, Volume 320, pages 97-124. doi 10.2475/02.2020.01

Christie, A.M.
1950: Geology of Bonavista map-area, Newfoundland (summary account). Department of Mines and Technical Surveys, Geological Survey of Canada, Paper 50-7, 40 pages.

Cocks, L.R.M. and Fortey, R.A.
2009: Avalonia: a long-lived terrane in the Lower Palaeozoic? *In* Early Palaeozoic Peri-Gondwana Terranes: New Insights from Tectonics and Biogeography. *Edited by* M.G. Bassett. Geological Society London, Special Publications 325, pages 141-155. doi 10.1144/SP325.7

Cohen, K.M., Finney, S.C., Gibbard, P.L. and Fan, J.-X.
2022: The ICS International Chronostratigraphic Chart. Episodes, Volume 36, pages 199-204.

Colman-Sadd, S.P., Hayes, J.P. and Knight, I.
1990: Geology of the Island of Newfoundland (digital version of Map 90-01); Scale: 1:1 000 000. Government of Newfoundland and Labrador, Department of Mines and Energy, Geological Survey Branch. Open File NFLD/2192.

Delor, C.P. and Rock, N.M.S.
1991: Alkaline-ultramafic lamprophyre dykes from the Vestfold Hills, Princess Elizabeth Land (East Antarctica): Primitive magmas of deep mantle origin. Antarctic Sciences, Volume 3, No. 4, pages 419-432.

Douglas, J.L.
1983: Geochemistry of the Cambrian manganese deposits of eastern Newfoundland. Unpublished Ph.D. thesis, Memorial University of Newfoundland, St. John's, Newfoundland, 305 pages.

Finch, C. Roldan, R., Walsh, L., Kelly, J. and Amor, S.
2018: Analytical methods for chemical analysis of geological materials. Government of Newfoundland and Labrador, Department of Natural Resources, Geological Survey, Open File NFLD/3316, 67 pages.

Fletcher, T.P.
2006: Bedrock geology of the Cape St. Mary's Peninsula, southwest Avalon Peninsula, Newfoundland, (includes parts of NTS map sheets 1M/1, 1N/4, 1L/16 and 1K/13). Government of Newfoundland and Labrador, Department of Natural Resources, Geological Survey, Report 06-02, 137 pages.

Floyd, P.A. and Winchester, J.A.
1975: Magma type and tectonic setting discrimination using immobile elements. Earth and Planetary Science Letters, Volume 27, pages 211-218.

Greenough, J.D.
1984: Petrology and geochemistry of Cambrian volcanic rocks from the Avalon Zone in Newfoundland and New Brunswick. Unpublished Ph.D. thesis, Memorial University of Newfoundland, St. John's, Newfoundland, 487 pages.

Greenough, J.D. and Papezik, V.S.
1985a: Petrology and geochemistry of Cambrian volcanic rocks from the Avalon Zone, Newfoundland. Canadian Journal of Earth Sciences, Volume 22, pages 1594-1601.

1985b: Chloritization of Cambrian volcanic rocks in eastern Newfoundland and southern New Brunswick, Canada. Chemical Geology, Volume 53, pages 53-70.

1986: Acado-Baltic volcanism in eastern North America and western Europe: Implications for Cambrian tectonism. Maritime Sediments and Atlantic Geology, Volume 22, pages 240-251.

Guiseppe, P.D., Agostini, S., Lustrino, M., Karaoglu, Ö., Savaşçin, M.Y., Manettie, P. and Ersoy, Y.
2018: Transition from compression to strike-slip tectonics revealed by Miocene-Pleistocene volcanism west of the Karliova Triple Junction (East Anatolia). Journal of Petrology, Volume 58, pages 2055-2087. https://doi.org/10.1093/petrology/egx082

Hayes, A.O.
1948: Geology of the area between Bonavista and Trinity bays, eastern Newfoundland. Geological Survey of Newfoundland, Bulletin 32 (Part 1), pages 1-37.

Henderson, B.J., Collins, W.J., Murphy, J.B., Gutiérrez-Alonso, G. and Hand, M.
2016: Gondwanan basement terranes of the Variscan–Appalachian orogeny: Baltican, Saharan and West African hafnium isotopic fingerprints in Avalonia, Iberia and the Armorican Terranes. Tectonophysics, Volume 681, pages 278-304.

Hibbard, J.P., van Staal, C.R., Rankin, D.W. and Williams, H.
2006: Lithotectonic map of the Appalachian Orogen, Canada-United States of America: Scale 1:1 500 000. Geological Survey of Canada Maps, 02096A.

Hiscott, R.N.
1982: Tidal deposits of the Lower Cambrian Random Formation, eastern Newfoundland: Facies and paleoenvironments. Canadian Journal of Earth Sciences, Volume 19, pages 2028-2042.

Howell, B.F.
1925: The faunas of the Cambrian *Paradoxides* beds at Manuels, Newfoundland. Bulletins of American Paleontology, Volume 11, No. 43, 140 pages.

Hutchinson, R.D.
1953: Geology of Harbour Grace map-area, Newfoundland. Geological Survey of Canada, Memoir 275, 43 pages.

1962: Cambrian stratigraphy and trilobite faunas of southeastern Newfoundland. Geological Survey of Canada, Bulletin 88, 156 pages.

Jenness, S.E.
1963: Terra Nova and Bonavista map-areas, Newfoundland (2D E1/2 and 2C). Geological Survey of Canada, Memoir 327, 184 pages.

King, A.F.
1988: Geology of the Avalon Peninsula, Newfoundland (parts of 1K, 1L, 1M, 1N and 2C). Government of Newfoundland and Labrador, Department of Mines and Energy, Geological Survey, Map 88-01.

Kuiper, Y.D., Murray, D.P., Ellison, S. and Crowley, J.L.
2022: U-Pb detrital zircon analysis of sedimentary rocks of the southeastern New England Avalon terrane in the U.S. Appalachians: Evidence for a separate crustal block. *In* New Developments in the Appalachian-Caledonian-Variscan Orogen. *Edited by* Y.D. Kuiper, J.B. Murphy, R.D. Nance, R.A. Strachan and M.D. Thompson. Geological Society of America, Special Paper 554, pages 1-27. https://doi.org/10.1130/2021.2554(05).

Landing, E.
1994: Precambrian-Cambrian boundary global stratotype ratified and a new perspective of Cambrian time. Geology, Volume 22, pages 179-782.

1996: Avalon: Insular continent by the latest Precambrian. *In* Avalonian and Related Peri-Gondwanan Terranes of the Circum-North Atlantic. *Edited by* R.D. Nance and M.D. Thompson. Geological Society of America, Special Paper 304, pages 29-63.

2004: Precambrian-Cambrian boundary interval deposition and the marginal platform of the Avalon microcontinent. Journal of Geodynamics, Volume 37, pages 411-435.

Landing, E., Geyer, G., Schmitz, M.D., Wotte, T. and Kouchinsky, A.
2021: (Re)proposal of three Cambrian Subsystems and their geochronology. International Union of Geological Sciences. Episodes 2021, Volume 41, pages 273-283. https://doi.org/10.18814/epiiugs/2020/020088

Landing, E., Westrop, S.R. and Geyer, G.
2022: Trans-Avalonian green–black transition (early Middle Cambrian): transform fault-driven epeirogeny and onset of 26 m.y. of shallow-marine, black mudstone in Avalonia (Rhode Island–Belgium) and Baltica. Canadian Journal of Earth Sciences. doi 101139/cjes-2022-0065

Large, R.R., Gemmell, J.B., Paulick, H. and Huston, D.L.
2001: The alteration box plot: a simple approach to understanding the relationships between alteration mineralogy and lithogeochemistry associated with volcanic-hosted massive sulphide deposits. Economic Geology, Volume 96, pages 957-971.

Lehnert, K., Su, Y., Langmuir, C., Sarbas, B. and Nohl, U.
2000: A global geochemical database structure for rocks. Geochemistry Geophysics Geosystems 1, Paper number 1999GC000026.

Macdonald, R., Rogers, N., Fitton, J.G. and Black, S.
2001: Plume-lithosphere interactions in the generation of the basalts of the Kenya Rift, East Africa. Journal of Petrology, Volume 42, pages 877-900.

Martin, F. and Dean, W.T.
1981: Middle and Upper Cambrian and Lower Ordovician acritarchs from Random Island, eastern Newfoundland. Geological Survey of Canada, Bulletin 343, 30 pages.

1988: Middle and Upper Cambrian acritarch and trilobite zonation at Manuels River and Random Island, eastern Newfoundland. Geological Survey of Canada, Bulletin 381, 91 pages.

Matthews, J.J., Liu, A.G., Yang, C., McIlroy, D., Levell, B. and Condon, D.J.
2020: A chronostratigraphic framework for the rise of the Ediacaran macrobiota: New constraints from Mistaken Point Ecological Reserve, Newfoundland. Geological Society of America, Bulletin 133, No. 3-4, pages 612-624.

Matton, G. and Jébrak, M.
2009: The Cretaceous Peri-Atlantic Alkaline Pulse (PAAP): Deep mantle plume origin or shallow lithospheric break-up? Tectonophysics, Volume 469, pages 1-12.

McCartney, W.D.
1955: Argentia map-area, Newfoundland (map sheet 1N/5). Geological Survey of Canada, Preliminary Map.

1956: Dildo map-area, Newfoundland (map sheet 1N/12). Geological Survey of Canada, Preliminary Map.

1958: Sunnyside map-area, Newfoundland (map sheet 1N/13). Geological Survey of Canada, Preliminary Map.

1967: Whitbourne map-area, Newfoundland. Geological Survey of Canada, Memoir 341, 135 pages.

Menzies, M. and Seyfried, W.E. Jr.
1979: Basalt-seawater interaction, trace element and strontium isotopic variations in experimentally altered glassy basalt. Earth and Planetary Science Letters, Volume 44, pages 463-472.

Miller, H.G. and Singh, V.
1995: The Avalon Terrane of Newfoundland: Geophysical correlations from onshore to offshore as evidence for Precambrian to Tertiary structural evolution. Tectonophysics, Volume 242, pages 183-197.

Mills, A.J.
2017: Depositional settings and tectonic evolution of rocks of the Bonavista Peninsula: New constraints and queries for Avalonia. Geological Association of Canada – Newfoundland Branch Fall Fieldtrip Guidebook, 66 pages.

2022: Reconnaissance-level lithogeochemical sampling of igneous rocks from the Avalon Terrane, eastern Newfoundland (NTS map areas 1M/3, 10, 1N/5, 6, 10, 11 and 12). Government of Newfoundland and Labrador, Department of Industry, Energy and Technology, Geological Survey, Open File NFLD/3414, 8 pages.

Mills, A.J., Dunning, G. and Sandeman, H.
2021: Age-constrained arc- to rift-magmatism in northwestern and central Avalon Terrane, Newfoundland, and implications for lithostratigraphy. Canadian Journal of Earth Sciences. doi 10.1139/cjes-2019-0196

Mills, A.J. and Sandeman, H.A.
2021a: Lithostratigraphy and lithogeochemistry of Ediacaran alkaline basaltic rocks of the Musgravetown Group, Bonavista Peninsula, northeastern Newfoundland, Canada: An extensional volcanogenic basin in the type-Avalon terrane. Atlantic Geology, Volume 57, pages 207-234.

2021b: Reconnaissance lithogeochemical investigation of the Bull Arm Formation and significance of diamictite in the overlying Big Head Formation in the Long Harbour–Placentia area, western Avalon Peninsula, Newfoundland. *In* Current Research. Government of Newfoundland and Labrador, Department of Industry, Energy and Technology, Geological Survey, Report 21-1, pages 73-96.

Miranda, R., Valladares, V., Terrinha, P., Mata, J., do Rosário Azevedo, M., Gaspar, M., Kullberg, J.C. and Riberiro, C.
2009: Age constraints on the Late Cretaceous alkaline magmatism on the West Iberian Margin. Cretaceous Research, Volume 30, pages 575-586.

Mohn, G., Manatschal, G., Beltrando, M., Masini, E. and Kusznir, N.
2012: Necking of continental crust in magma-poor rifted margins: Evidence from the fossil Alpine Tethys margins. Tectonics, Volume 31. doi 10.1029/2011TC002961

Murphy, J.B., Gutiérrez-Alonso, G., Nance, R.D., Fernández-Suárez, J., Keppie, J.D., Quesada, C., Dostal, J. and Braid, J.A.
2009: Rheic Ocean mafic complexes: overview and synthesis. *In* Ancient Orogens and Modern Analogues. *Edited by* J.B. Murphy, J.D. Keppie and A.J. Hynes. Geological Society of London, Special Publications 327, pages 343-369.

Murphy, J.B. and Nance, R.D.
1989: Model for the evolution of the Avalonian-Cadomian belt, Geology, Volume 17, pages 735-738.

Murphy, J.B., Pisarevsky, S.A., Nance, R.D. and Keppie, J.D.
2004: Neoproterozoic-Early Paleozoic evolution of peri-Gondwanan terranes: Implications for Laurentia-Gondwana connections. International Journal of Earth Sciences, Volume 93, pages 659-682.

Nance, R.D., Murphy, J.B., Strachan, R.A., Keppie, J.D., Gutiérrez-Alonso, G., Fernández-Suárez, J., Quesada, C., Linnemann, U., D'Lemos, R. and Pisarevsky, S.A.
2008: Neoproterozoic-early Palaeozoic tectonostratigraphy and palaeogeography of the peri-Gondwanan terranes: Amazonian v. West African connections. *In* The Boundaries of the West African Craton. *Edited by* N. Ennih and J.-P. Liégeois. Geological Society, London, Special Publications 297, pages 345-383.

Narbonne, G.M., Laflamme, M., Greentree, C. and Trusler, P.
2009: Reconstructing a lost world: Ediacaran rangeomorphs from Spaniard's Bay, Newfoundland. Journal of Paleontology, Volume 83, No. 4, pages 503-523. http://www.jstor.org/stable/29739123

Niu, Y., Wilson, M., Humphreys, E.R. and O'Hara, M.J.
2011: The origin of intra-plate Ocean Island Basalts (OIB): the lid effect and its geodynamic implications. Journal of Petrology, Volume 52, Nos. 7-8, pages 1443-1468.

Normore, L.S.
2010: Geology of the Bonavista map area (NTS 2C/11), Newfoundland. *In* Current Research. Government of Newfoundland and Labrador, Department of Natural Resources, Geological Survey, Report 10-1, pages 281-301.

2011: Preliminary findings on the geology of the Trinity map area (NTS 2C/06), Newfoundland. *In* Current Research. Government of Newfoundland and Labrador, Department of Natural Resources, Geological Survey, Report 11-1, pages 273-293.

O'Brien, S.J.
1994: On the geological development of the Avalon Zone in the area between Ocean Pond and Long Islands, Bonavista Bay (parts of NTS 2C/5 and NTS 2C/12). *In* Current Research. Government of Newfoundland and Labrador, Department of Mines and Energy, Geological Survey Branch, Report 94-1, pages 187-199.

Pearce, J.A.
1996: A user's guide to basalt discrimination diagrams. *In* Trace Element Geochemistry of Volcanic Rocks; Applications for Massive Sulphide Exploration. Short Course Notes, Geological Association of Canada, Volume 12, pages 79-113.

2008: Geochemical fingerprinting of oceanic basalts with applications to ophiolite classification and the search for Archean oceanic crust. Lithos, Volume 100, pages 14-48.

Pe-Piper, G., Meredyk, S., Zhang, Y., Piper, D.J.W. and Edinger, E.
2013: Petrology and tectonic significance of seamounts within transitional crust east of Orphan Knoll, offshore eastern Canada. Geo-Marine Letters, Volume, 33, pages 433-447.

Pollock, J.C., Hibbard, J.P. and Sylvester, P.J.
2009: Ordovician rifting of Avalonia and birth of the Rheic Ocean: U-Pb detrital zircon constraints from Newfoundland. Journal of the Geological Society, London, Volume 166, pages 501-515.

Pollock, J.C., Hibbard, J.P. and van Staal, C.R.
2012: A paleogeographical review of the peri-Gondwanan realm of the Appalachian orogeny. Canadian Journal of Earth Sciences, Volume 49, pages 259-288.

Poulsen, V. and Anderson, M.M.
1975: The Middle-Upper Cambrian transition in southeastern Newfoundland, Canada. Canadian Journal of Earth Sciences, Volume 12, pages 2065-2079.

Pu, J.P., Bowring, S.A., Ramezani, J., Myrow, P., Raub, T.D., Landing, E., Mills, A., Hodgin, E. and Macdonald, F.A.
2016: Dodging snowballs: Geochronology of the Gaskiers glaciation and the first appearance of the Ediacaran biota. Geology, Geological Society of America, Data Repository item 2016326, 4 pages. doi 10.1130/G38284.1

Ringwood, A.E.
1975: Composition and petrology of the Earth's mantle. McGraw-Hill Book Co., New York, N.Y., USA, 618 pages.

Roeder, P.L. and Emslie, R.F.
1970: Olivine-liquid equilibrium. Contributions to Mineralogy and Petrology, Volume 29, pages 275-289.

Rooney, T.O.
2010: Geochemical evidence of lithospheric thinning in the southern Main Ethiopian Rift. Lithos, Volume 117, pages 33-48.

Sun, S.-S. and McDonough, W.F.
1989: Chemical and isotopic systematics of oceanic basalts: Implications for mantle composition and

processes. *In* Magmatism in the Ocean Basins. *Edited by* A.D. Saunders and M.J. Norry. Geological Society of London, Special Publication 42, pages 313-345.

Thompson, M.D., Barr, S.M. and Grunow, A.M.
2012: Avalonian perspectives on Neoproterozoic paleogeography: Evidence from Sm-Nd isotope geochemistry and detrital zircon geochronology in SE New England, USA. Geological Society of America, Bulletin 124, pages 517-531. https://doi.org/10.1130/B30529.1

Thompson, M.D., Barr, S.M. and Pollock, J.C.
2022: Evolving views of West Avalonia: Perspectives from southeastern New England, USA. *In* New Developments in the Appalachian-Caledonian-Variscan Orogen. *Edited by* Y.D. Kuiper, J.B. Murphy, R.D. Nance, R.A. Strachan and M.D. Thompson. Geological Society of America, Special Paper 554, pages 47-72. https://doi.org/10.1130/2022.2554(03).

van Staal, C.R.
2007: Pre-Carboniferous tectonic evolution and metallogeny of the Canadian Appalachians. *In* Mineral Deposits of Canada: A Synthesis of Major Deposit-Types, District Metallogeny, the Evolution of Geological Provinces, and Exploration Methods. *Edited by* W.D. Goodfellow. Geological Association of Canada, Mineral Deposits Division, Special Publication No. 5, pages 793-818.

van Staal, C.R., Barr, S.M., McCausland, P.J.A., Thompson, M.D. and White, C.E.
2020: Tonian–Ediacaran tectonomagmatic evolution of West Avalonia and its Ediacaran–early Cambrian interactions with Ganderia: An example of complex terrane transfer due to arc-arc collision? *In* Pannotia to Pangaea: Neoproterozoic and Paleozoic Orogenic Cycles in the Circom-Atlantic Region. *Edited by* J.B. Murphy, R.S. Strachan and C. Quesada. Geological Society of London, Special Publications 503, pages 143-167.

Wilson, J.T.
1966: Did the Atlantic close and then re-open? Nature, Volume 211, pages 676-681.